Astron. Astrophys. 253, 150–172 (1992)

ASTRONOMY AND ASTROPHYSICS

# A flux-limited sample of galactic carbon stars

**M.A.T. Groenewegen[1], T. de Jong[1,2], N.S. van der Bliek[3], S. Slijkhuis[1], and F.J. Willems[1]**

[1] Astronomical Institute 'Anton Pannekoek', Kruislaan 403, NL-1098 SJ Amsterdam, The Netherlands
[2] SRON, P.O. Box 800, NL-9700 AV Groningen, The Netherlands
[3] Sterrewacht Leiden, P.O. Box 9513, NL-2300 RA Leiden, The Netherlands

Received December 18, 1990; accepted June 13, 1991

**Abstract.** We have studied an infrared-complete sample of bright carbon stars containing all 109 carbon stars with $S_{12} > 100$ Jy in the IRAS PSC. This sample is more complete than others previously studied, in that both optical and infrared carbon stars are included.

Using near-infrared photometry from the literature we derived near-infrared colour temperatures and using the full energy distribution we calculated infrared bolometric corrections. Distances were derived assuming $M_{bol} = -4.9$, corresponding to $L = 7050 L_{\odot}$. From the available CO data the mass loss rates were calculated for about 80 stars in this sample.

The sample was divided into five groups depending upon their infrared properties, extending the classification of carbon stars of Willems & de Jong (1988). Group I stars show the silicate feature in their LRS spectra, possibly because they are very recently formed carbon stars. Group II stars have a pronounced 60 μm excess, high near-infrared temperatures, small bolometric correction and low mass loss rates. They probably turned into a carbon star quite recently and their excess at 60 μm is due to a cool circumstellar shell, the remnant of the preceding high mass loss phase. From group III to V the mass loss rate of carbon stars steadily increases and, as a consequence, the near-infrared temperatures decrease and the bolometric corrections increase.

Using the average bolometric corrections for each group the infrared-complete sample is transformed into a volume-complete one. The scale height of carbon stars is 190 pc and the local space density of carbon stars equals 185 $kpc^{-3}$.

From the calculated space densities of carbon stars in each group relative timescales are derived. Adopting a lifetime of 20 000 years for group II stars from model calculations, we find a total lifetime of the carbon star phase of about 26 000 years, uncertain to a factor of 2. We have compared our carbon star number densities and timescales with the death rate of their likely progenitors on the main sequence and their descendants, the carbon-rich PN. At face value both comparisons would indicate that the lifetimes derived by us are too short. However, taking into account the uncertainties in both timescales and in the death rate and birth rate history of the main sequence stars, both values are not inconsistent. The agreement can be improved if we assume that not all carbon stars evolve into carbon-rich PN. We briefly discuss two possibilities: Hot bottom envelope burning (HBB) which may transform a carbon star back into an oxygen-rich star and termination of the AGB at such a low core mass that the evolution to the left in the HR diagram is too slow for PN formation. It is also possible that the number density of PN is larger than usually assumed.

The total mass lost during the carbon star phase is only $0.04 M_{\odot}$. This number is uncertain to a factor of 5, a factor 2 arising from the uncertainty in the lifetime of group II stars and a factor 2.5 arising from the uncertainty in the mass loss rates. If we assume an average white dwarf mass of $0.65 M_{\odot}$, our results imply that most stars are already of low mass when they turn into carbon stars, probably around $0.69 M_{\odot}$ and certainly less than $0.87 M_{\odot}$. We conclude that a "superwind" phase, if it exists, should last for less than approximately 20 yr.

**Key words:** infrared radiation: stars – bolometric correction: stars – carbon: stars – evolution: stars – mass loss

## 1. Introduction

With the advent of infrared and radio techniques it has become clear that carbon stars do not only manifest themselves in the photospheric spectrum – the classical method to identify a carbon star – but also in the circumstellar shell surrounding the star. Most carbon stars show a spectral feature around 11.3 μm which is attributed to silicon carbide (SiC), while oxygen-rich M stars usually show the silicate feature around 9.7 μm.

One can distinguish between two kinds of carbon stars, the "optical" carbon stars, identified through their optical spectra, and the "infrared" carbon stars, displaying the SiC feature but often without known optical counterpart. Although identified by different means, both classes represent carbon stars, and so their relation should be carefully examined. Do they e.g. represent an evolutionary sequence?

An attempt to put the carbon stars in an evolutionary scheme using IRAS data was made by Willems & de Jong (1986, 1988, see also Willems 1988a, b) who studied the infrared properties of a sample of about 300 opticaly known carbon stars for which LRS spectra were available. Using a subsample of 90 stars for which reliable near-infrared photometry was available at the time, they divided their sample into three groups. Group I consisted of 9 objects known to be carbon stars from their optical spectra but displaying the 9.7 μm silicate feature in emission, commonly found exclusively in oxygen-rich stars (Willems & de Jong 1986; Little-Marenin 1986). The remaining stars were divided into group II, characterised by a near-infrared colour temperature $T_{nir} > 2000$ K, and group III with $T_{nir} < 2000$ K.

A scenario for carbon star evolution explaining the relation

*Send offprint requests to*: M. Groenewegen

between the three groups of stars was given by Willems & de Jong (1988). This scenario runs as follows. During asymptotic giant branch (AGB) evolution, regularly pulsating M Mira variables produce a circumstellar silicate dust shell. Presumably triggered by a thermal pulse, carbon becomes more abundant than oxygen in the photosphere and the star turns into a carbon star. This transition seems to be accompanied by a sharp decrease in the mass loss rate. The circumstellar shell is no longer replenished and, thus, expands and dilutes. As it expands the dust shell cools and, as a consequence, the star will describe a loop in the IRAS colour–colour diagram. While the last oxygen-rich material moves out, a new carbon-rich circumstellar shell is beginning to form. At first, the mass loss rate is low, but when the star becomes a carbon Mira the mass loss rate will increase to a typical value of $\sim 10^{-6} M_{\odot}$/yr. In this scenario the group I stars represent the stars which very recently underwent the transition of oxygen to carbon star, so that their circumstellar shell has not diluted yet and the silicate feature can still be seen in the LRS spectrum. Group II represents stars which have almost completed their loop in the colour–colour diagram. They show a far-infrared excess, but their near-infrared spectra are dominated by the stellar continuum. Group III represent stars in which carbon-rich dust is beginning to mask the stellar continuum at near-infrared wavelengths.

Although the identification of group I stars with objects that recently underwent the rapid transition of oxygen to carbon star is still controversial, and alternative explanations have been proposed (see e.g. Little-Marenin 1986; Benson & Little-Marenin 1987; Zuckerman & Maddalena 1989; de Jong 1989; Le Bertre et al. 1990; Deguchi et al. 1990; Lloyd Evans 1990; Lambert et al. 1990 and Skinner et al. 1990 for recent discussions on the nature of group I stars), the general idea of an expanding shell after the transition of oxygen to carbon star remains unchallenged. Based on simple model calculations, Willems & de Jong (1988) could well explain the position of the group II stars in the IRAS colour–colour diagram. Their results were confirmed by more elaborate calculations by Chan & Kwok (1988).

In this paper we use the terminology of Willems & de Jong (1988). In addition we introduce groups IV and V. It was suggested by Willems (1988b) that the group III stars would ultimately evolve into AFGL carbon stars, like IRC+10216, carbon Miras obscured by their circumstellar shell. As they represent a more evolved state in the evolution of carbon stars this group will be denoted as group IV. Finally, we introduce group V stars representing the latest stage of carbon star evolution.

The aim of this paper is to investigate the properties of a complete flux-limited sample of galactic carbon stars. Similar studies were undertaken by Claussen et al. (1987), Thronson et al. (1987), Willems & de Jong (1988), Jura et al. (1989) and Jura & Kleinmann (1989). These authors, however, studied only partially complete samples of carbon stars. Claussen et al. studied the carbon stars found in the "Two Micron Sky Survey" (TMSS; Neugebauer & Leighton 1969) and, therefore, missed the carbon stars with thick circumstellar shells. Thronson et al. selected carbon stars from a box in the IRAS colour–colour diagram with $-0.66 \leq \log(S_{25}/S_{12}) \leq -0.38$ and $-0.68 \leq \log(S_{60}/S_{25}) \leq -0.0$.[1] After removing known oxygen-rich stars Thronson et al. still estimated a contamination of 7% oxygen-rich stars in their sample. Furthermore, they used a correction factor of 25% to correct for carbon stars outside the box they considered. From this study we actually find that about 40% of the carbon stars are outside the box considered by Thronson et al. Willems & de Jong (1988) studied the optical carbon stars found in the "IRAS Low Resolution Spectrograph" atlas (LRS atlas; Joint IRAS Science Working Group 1986). Jura & Kleinmann studied dust-enshrouded AGB stars within 1 kpc from the sun and Jura et al. studied the carbon stars in the direction of the galactic anticentre found in the survey by Fuenmayor (1981).

The paper is organised as follows. In Sect. 2 we discuss the selection of the sample. Depending upon their infrared properties the sample is divided into 5 groups in Sect. 3. In Sect. 4 bolometric corrections are calculated. These are used to transform our flux-limited sample into a volume-complete one. In Sect. 5 mass loss rates are derived from CO measurements and, finally, in Sect. 6 an evolutionary sequence for carbon star evolution is presented and evolution timescales and the total mass lost in the carbon star phase are derived.

## 2. The sample

Our flux-limited sample of galactic carbon stars consists of all carbon stars with a 12 μm flux density larger than 100 Jy, as listed in the "IRAS Point Source Catalog" (PSC; Joint IRAS Science Working Group 1986) version 2.0. This rather large limiting flux density was chosen to ensure that our sample is complete (at least over the 95% of the sky covered by the PSC). An additional advantage of this choice is that NIR and CO data, which are needed for our analysis, are only available for the IR brightest stars.

The 610 stars in the PSC with $S_{12} > 100$ Jy can be divided into those which have a spectrum in the LRS atlas and those without a spectrum in the LRS atlas. In our search for carbon stars with $S_{12} > 100$ Jy we will first consider the former category.

As already stated in the introduction, it has become clear that carbon stars can be identified both based on their optical spectra and on their infrared spectral features. Since we want to construct a complete sample, both methods of finding carbon stars should be employed. We will first search for carbon stars with $S_{12} > 100$ Jy in the optical surveys and than consider the infrared carbon stars.

The largest single collection of optically identified carbon stars is still the "General Catalogue of Cool Carbon Stars" (GCCCS; Stephenson 1973).[2] Since then many new discoveries

[1] In this paper we denote flux densities by $S_\lambda$ (in units of Jy or erg/s/cm$^2$/Hz) or, if we prefer the same quantity in wavelength units (W/m$^2$/μm), by $F_\lambda$. The subscript indicates the wavelength (μm) at which $S_\lambda$ and $F_\lambda$ are evaluated. The total or integrated fluxes, i.e. $F_\lambda$ (or $S_\lambda$) integrated over wavelength (or frequency) will be denoted by $F$ (or $S$) without subscript.

[2] When our analysis was completed, we became aware of the second edition of the GCCCS (Stephenson 1989), which contains information on about 5800 carbon stars identified from optical spectra and some 180 infrared carbon stars from Little-Marenin et al. (1987). We have used the first edition of the GCCCS listing 3300 stars and about 1700 stars from additional references (see below). The new deep surveys conducted since 1973 only list very few bright carbon stars. From the 39 optical carbon stars found, 34 are listed in the GCCCS and only 5 come from the additional references. Our procedure for selecting an infrared complete sample of carbon stars is independent of the choice of the optical carbon star catalogue.

have been reported. Willems & de Jong (1986) correlated the stars listed in the GCCCS, and the new discoveries reported by Alksne & Ozolina (1972, 1974, 1975, 1976, 1983), Daube & Ozolina (1974), Alksnis et al. (1976, 1977, 1978), MacConnell (1979, 1982), Kurtanidze & West (1980), Fuenmayor (1981) and Stephenson (1985), altogether about 3750 stars, with the LRS atlas. They found 304 associations. Thirty-six of these have $S_{12}>100$ Jy. Since then more newly discovered optical carbon stars have been reported by e.g. Maehara & Soyano (1987a, b, 1988), Nikolashvili (1987a, b), Alknis et al. (1988), MacConnell (1988), Sanduleak & Pesch (1988), Kurtanidze & Nikolashvili (1988, 1989) and Aaronson et al. (1989, 1990). These, about 1200 new discoveries, were correlated on position with the PSC. Although about 580 entries were found in the PSC, only 35 are listed in the LRS atlas and only 3(all listed by MacConnell) have $S_{12}>100$ Jy. So, from the optical surveys we find 39 carbon stars with $S_{12}>100$ Jy, listed in the LRS atlas.

Infrared carbon stars were selected from the PSC by taking all sources with $S_{12}>100$ Jy and a 4n classification (indicating the presence of the SiC feature) in the LRS atlas. This resulted in a sample of 92 candidate carbon stars. This sample included 37 of the 39 carbon stars already selected from the optical surveys. One well-known S-stars ($\pi$ $^1$Gru) was removed from the sample.

The LRS spectra of the remaining 54 sources were inspected by eye to check if they indeed showed the 11.3 μm feature, because it is known that some oxygen-rich stars with the 9.7 μm feature in absorption have been misclassified as 4n (cf. Walker & Cohen 1988). Nine stars that clearly show the 9.7 μm feature (and the 18 μm feature) but have been misclassified as 4n in the LRS atlas are listed in Table 1. Seven of them have independently been classified as oxygen-rich from optical spectra or are known OH-sources.

To allow for the possibility that some infrared carbon stars have *not* been classified as 4n, we inspected the LRS spectra of all 518 non-4n sources brighter than 100 Jy to search for the SiC feature. Four additional infrared carbon stars were found. Among them were the well-known objects AFGL 865 and IRAS 15194−5115 (Maedows et al. 1987). Thus, the number of true infrared carbon stars extracted from the LRS atlas is 49.

From the infrared carbon stars for which an optical spectrum is available we find that about one in forty stars with a 4n classification is an S-star. It is thus possible that among the 49 infrared carbon stars in our sample about one could be an S-star. This will not influence our analysis significantly.

**Table 1.** Misclassified 4n objects with $S_{12}>100$ Jy

| IRAS name | Association |
|---|---|
| 04530+4427 | NIPPS 392 C7 (M5 III) |
| 14582−5926 | OH source (te Lintel Hekkert 1990) |
| 15492+4837 | ST Her (M6 III aS); AFGL 5313; IRC+50247; SAO 45758 (MC) |
| 17360−3012 | AFGL 1992; OH358.16+0.49 |
| 17371−3021 | OH-source (Le Squeren et al. 1990) |
| 17482−2824 | AFGL 5146S; OH source (Le Squeren et al. 1990) |
| 18092−0437 | AFGL 2088 |
| 18135−1740 | AFGL 2102; IRC−20455 (M3) |
| 18333+0533 | AFGL 2199; NIR colours similar to OH/IR stars (Whitelock 1985) but not detected in OH (Eder et al. 1988) |

The LRS atlas is less complete than the PSC. Even at high galactic latitudes it contains only 90% of the point sources brighter than 28 Jy at 12 μm (Hacking et al. 1985). This implies that there are carbon stars with $S_{12}>100$ Jy that are not listed in the LRS atlas but which should be included in our sample. Fortunately, however, Volk & Cohen (1989) recently presented the low-resolution spectra of all 356 sources brighter than 40 Jy at 12 μm not listed in the LRS atlas. They extracted these spectra directly from the LRS database. Most sources lie in the galactic plane. Instead of using the same criteria as was done in the LRS atlas to classify each spectrum by assigning a two-number code, Volk & Cohen used there own one-letter code to classify each spectrum. For example, a spectrum showing the SiC feature was classified as "C", a spectrum clearly resembling a stellar blackbody as "S" and a featureless spectrum expected to be a star with small amounts of circumstellar material as "F". Volk & Cohen list 29 carbon stars, 11 of which are listed in the GCCCS and 18 without known optical counterpart. Sixteen have $S_{12}>100$ Jy. Two of them (IRAS 17512−2548 and 18288−0837) have an unreliable 60 μm flux and were no longer considered. The remaining 14 were added to our sample. Among them is the well-known carbon star TX Psc. Volk & Cohen classified 13 of them as "C" and one (TX Psc) as "S".

Plotting the 102 stars so far selected in the IRAS colour–colour diagram we noticed that the reddest carbon stars extended only to $C_{21}=2.5\log(S_{25}/S_{12})\approx 0.0$, while their oxygen-rich counterparts on the AGB, the OH/IR stars, are known to extend up to $C_{21}\approx 2$ (te Lintel-Hekkert 1990). On the other hand, some carbon stars are known to have $C_{21}>0.0$, e.g. AFGL 3068($C_{21}=0.10$; Jones et al. 1978) and AFGL 190 ($C_{21}=0.42$; Kleinmann et al. 1981; Zuckerman & Dyck 1986). Their LRS spectra are almost featureless. To find more of these very red carbon stars we inspected by eye all 79 LRS spectra with $S_{12}>100$ Jy, a non-4n classification and $C_{21}\geq -0.25$ and $C_{32}\geq -2.0$. After removing all stars associated with oxygen-rich objects and young stars, we were left with 7 likely and 1 possible carbon star. These stars are discussed in more detail in Sect. 3. Volk & Cohen (1989) list another 2 featureless "F" sources without association but they have $S_{12}<100$ Jy as well as $C_{21}<-0.25$ and, therefore, did not make it into our sample.

In summary, our sample consists of 109 certain and 1 possible carbon star. We will denote this sample as the infrared bright carbon star sample (IBCSS).

## 3. The division of the IBCSS into different groups

In this section our sample of 109 stars will be divided into groups. As discussed in Sect. 2, Willems & de Jong (1988a, b) discriminated between groups II and III using the value of $T_{\rm nir}$. All objects with $T_{\rm nir}>2000$ K were assigned by them to group II. We also found this to be a very useful criterion (see Table 2). From the values of the bolometric correction (details to be discussed in the following section) in column 6 of Table 2 and Fig. 2 it is striking to see that all group II objects, except one, have distinctly lower bolometric corrections than members of the other groups. In fact, this observation helped us in some cases, when $T_{\rm nir}$ was close to 2000 K, to assign a source to group II. Another characteristic

that distinguishes between group II and group III is their position in the colour–colour diagram. Group II objects have a 60 μm excess, while group III objects cluster around the blackbody line. A characteristic that group II and group III have in common, contrary to the infrared carbon stars, is the presence of a known optical counterpart, i.e. listed in the GCCCS or another objective prism survey, in the "General Catalogue of Variable stars" (GCVS, Kholopov et al. 1985) or in the "New Catalogue of Suspected Variable Stars" (NSV, Kukarkin et al. 1982). For the division of our sample we used the following four criteria: the presence of an optical counterpart, position in the colour–colour diagram, near-infrared colour temperatures and infrared bolometric corrections.

In Fig. 1 all stars are plotted in an IRAS colour–colour diagram. We use $C_{21}=2.5\log(S_{25}/S_{12})$ and $C_{32}=2.5\log(S_{60}/S_{25})$ as variables. The fluxes listed in the PSC were colour-corrected in the same way as was done by Willems & de Jong (1986), i.e. the $C_{21}$ colour was used to correct the 12 μm flux and $C_{32}$ to correct the 25, 60 and 100 μm flux densities using Table VI.C.6 in the "Explanatory Supplements" (Joint IRAS Science Working Group 1988).

In Table 3 we list associations with sources in several important catalogues.

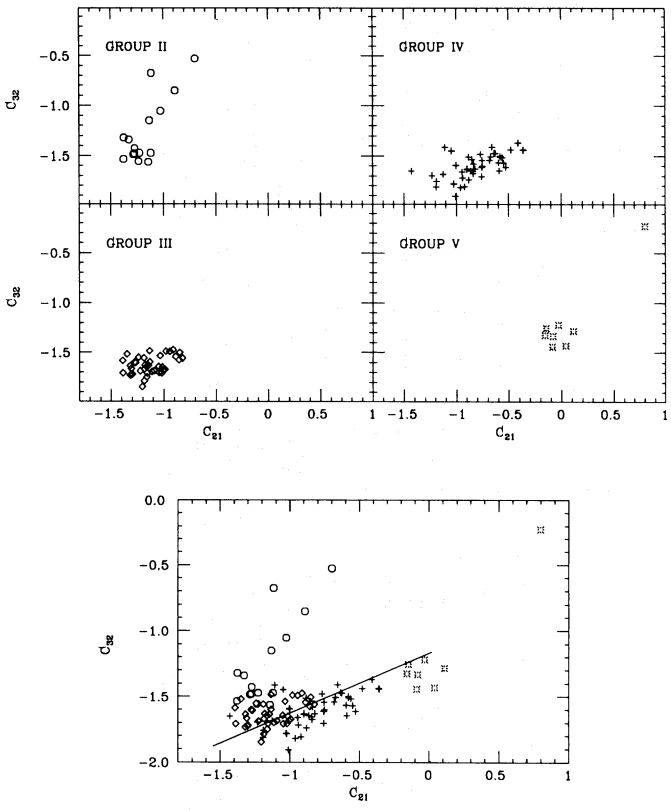


**Fig. 1.** The position of the IBCSS stars in the IRAS colour–colour diagram. In the top four figures the sample is separated into the different groups. In the bottom figure the total sample is plotted. The solid line indicates the location of the blackbody line

### 3.1. Group I

None of the nine stars proposed by Willems & de Jong (1986) and Little-Marenin (1986) to be carbon stars with silicate dust shells have made it into our sample.

Willems & de Jong already noted that the association of C2123 with IRAS 13442−6109, the only group I star with $S_{12}>100$ Jy, was uncertain (a difference between the optical and infrared position of 100″). Recently, it was confirmed (Le Bertre et al. 1990) that the true optical counterpart of IRAS 13442 −6109 is not C2123 but an oxygen-rich star.

We will briefly return to the evolutionary status of the group I stars in Sect. 7.

### 3.2. Group II

Out of a total of 109 stars, 15 were classified as group II. One star, IRAS 20180+4744 (U Cyg), is a doubtful member. The near-infrared temperature is low (2290 K) for a group II star but well above 2000 K, and the bolometric correction (see Fig. 2) is high for a group II but low for a group III star. The position in the colour–colour diagram ($C_{21}=-1.24$, $C_{32}=-1.56$) slightly favours a group II classification, so this object was classified as group II.

For the stars in common with Willems (1988a) our near-infrared temperatures agree very well with his. The average difference is somewhat less than 50 K.

Some general characeristics of group II stars are:

— All have $BC_{12}<5.0$ (except U Cyg: $BC_{12}=5.51$)

— All have a known optical counterpart. IRAS 17314−3255 is listed by Fuenmayor (1981), all others are listed in the GCCCS and GCVS.

— The near-infared temperature ranges from 2260 K to 2820 K.

### 3.3. Group III

Thirty-nine stars were classified as group III. One dubious member, IRAS 19175−0807, has a near-infrared colour temperature well above 2000 K, unlike all other group III stars but has a bolometric correction and position in the colour–colour diagram characteristic of other group III stars. It was classified as a group III star.

Some general characteristics of group III stars are:

— Near-infrared colour temperatures range between 730 and 1920 K (except IRAS 19175−0807 with $T_{nir}=2630$ K), but only 4 have $T_{nir}<1000$ K, the second lowest being 940 K.

— Bolometric corrections range from 5.2 to 8.4, but most (90%) have $BC_{12}<7.4$. There is considerable overlap with group IV stars but for $BC_{12}<6.6$ all stars belong to group III.

— All are listed in the GCCCS, the GCVS or the NSV.

### 3.4. Group IV

The majority of stars in the sample were assigned to this group, 48 in all. One star, IRAS 03186+7016 (AFGL 482), has an unusual high near-infrared temperature, typical of a group II star, but its position near the blackbody line is typical for a group IV star and so it was assigned to group IV.

Some general characteristics are:

— Bolometric corrections range from 6.6 to 8.6. There is considerable overlap with group III stars. Solely on the basis of $BC_{12}$ the two groups cannot be distinguished.

— The near-infrared temperatures are low, usually below 1000 K. Actually, a practical definition to separate group III and IV stars would be to use the criterion of $T_{\rm nir} \gtrless 1000$ K. In the present sample 11% of group III have $T_{\rm nir} < 1000$ K, while 11% of group IV have $T_{\rm nir} > 1000$ K.

— Very few are listed in the IRC, GCCCS or GCVS atlasses.

### 3.5. *Group V*

As explained in the previous section our effort to include the reddest carbon stars by inspecting by eye all 79 LRS spectra of sources with $S_{12} > 100$ Jy, $C_{21} \geq -0.25$, $C_{32} \geq -2.0$ and a non-4n LRS classification resulted in a sample of 7 likely and 1 possible carbon star. All these objects are classified as group V (since group IV objects extend to $C_{21} \approx 0.0$ and all group V objects happen to have $C_{21} > 0.0$, a more practical definition would be to define a group V object as an infrared carbon star with $C_{21} \geq 0.0$). All individual objects are briefly discussed below, first the seven likely, then the possible carbon star, in order of right ascension.

*IRAS 01144+6658*

Zuckerman & Dyck (1986b) classify this object (AFGL 190) as a carbon star based on its relative intense HCN line emission. The mere detection of HCN is not sufficient to classify a star as a carbon star because this molecule has also been detected in oxygen-rich stars (Lindqvist et al. 1988; Nercessian et al. 1989) but the ratio $T_{\rm mb}({\rm CO})/T_{\rm mb}({\rm HCN})$ can be used to discriminate between carbon-rich and oxygen-rich objects. The value for AFGL 190 indicates a carbon-rich nature. Kleinmann et al. (1981) also classify it as a carbon star.

*IRAS 04395+3601*

This object, better known as AFGL 618 is thought to be a proto-planetary nebula. It was studied in detail by Westbrook et al. (1975). Its spectrum is almost featureless, consistent with graphite (or amorphous carbon) being the dominant dust species in the circumstellar shell (Russell et al. 1978). It has been detected in many molecular transitions, e.g. $^{12}$CO, $^{13}$CO, HCN, CS, $C_3H_2$ (see Bujarrabal et al. 1988), confirming its carbon-rich nature. Although this object may no longer be on the AGB, Kwok & Bignell (1984) estimated it to have left the AGB less than 100 years ago, it was kept in our sample. It can be seen from Fig. 1 that it is the reddest object in our sample. Inspecting the LRS spectrum of this source, Lequeux & de Muizon (1990) conclude that the SiC feature is in absorption, implying a high mass loss rate.

*IRAS 08171−2134*

Independent evidence that this object (AFGL 5250) is indeed carbon-rich is given by Zuckerman & Dyck (1986b) who classify it as a carbon star because of its intense HCN emission.

*IRAS 17353−3030*

This star (AFGL 5416) is listed by Zuckerman & Dyck (1986b) as a possible carbon star.

*IRAS 19075+0921*

Zuckerman & Dyck (1986b) classify this star as a carbon star because of its strong HCN emission and because the LRS spectrum, according to them, shows weak SiC emission.

*IRAS 21318+5631*

An UKIRT spectrum taken on September 26, 1990 by one of us (MG) reveals the 3.1 μm feature atttribued to HCN and $C_2H_2$. This confirms the carbon richness of this source (see e.g. Merrill & Stein 1976 or Noguchi et al. 1977).[3]

Zuckerman et al. (1986) classify this object as oxygen-rich, but do this solely on the basis of the IRAS broad-band colours. Such a criterion for classification is clearly unjustified in this case because, as can been seen in Fig. 1, all group V objects (except the possible PPN AFGL 618) have very similar colours and are indeed *carbon*-rich.

*IRAS 23116+1655*

Jones et al. (1978) present 2–13 μm spectrophotometry for this star (AFGL 3068) that confirm it as being carbon-rich. The spectrum shows the 3.1 μm feature due to $C_2H_2$ and HCN and the spectrum near 10 μm suggests that the SiC feature is in absorption. This implies a high mass loss rate.

*IRAS 15471−5644*

This star was listed as a possible carbon stars because its LRS spectrum looks similar to the seven carbon stars discussed above. No independent evidence exists to support this claim. However, there is also no evidence to the contrary. Spectrophotometry in the 2–4 μm region and CO and HCN measurements would reveal the nature of this subject. We note that the feature near 11 μm in the LRS spectrum is not related to the SiC feature but probably a spike.

## 4. Bolometric corrections

In this section infrared bolometric corrections are calculated for our sample stars. We already used them in the previous section to help in disciminating between the different groups. Bolometric corrections are needed to convert a flux-limited sample into a volume-complete one.

Analogous to the optical definition the following definition is used:

$$M_{\rm bol} = M_{12\,\mu{\rm m}} + BC_{12}. \quad (1)$$

Using $M_{\rm bol} = 4.72$ for the sun and a zero-magnitude flux density of 28.3 Jy for the 12 μm band ("Explanatory Supplement", page VI-21), Eq. (1) can be written after some manipulation as

$$BC_{12} = -2.5 \log \frac{\int_0^\infty F_\lambda {\rm d}\lambda}{12\, F_{12}} + 8.86, \quad (2)$$

where $F_\lambda$ and $F_{12}$ are in W/m$^2$/μm and $\lambda$ is in μm. This equation is similar to the definition used by Herman et al. (1986) and van der Veen & Breukers (1989).

[3] This and other NIR spectra of candidade carbon stars will be published in a separate paper.

The integral over the observed spectral energy distribution may be separated as follows:

$$\int_0^\infty F_\lambda \mathrm{d}\lambda = C_{\mathrm{nir}}\left(\int_0^{\lambda_{\min}} B_\lambda(T_{\mathrm{nir}})\mathrm{d}\lambda + \int_{\lambda_{\min}}^{\lambda_1} B_\lambda(T_{\mathrm{nir}})\mathrm{d}\lambda\right) + \int_{\lambda_1}^{\lambda_2} F_\lambda \mathrm{d}\lambda + C_{\mathrm{fir}}\left(\int_{\lambda_2}^{\lambda_{\max}} B_\lambda(T_{\mathrm{fir}})\mathrm{d}\lambda + \int_{\lambda_{\max}}^{\infty} B_\lambda(T_{\mathrm{fir}})\mathrm{d}\lambda\right), \quad (3)$$

where $T_{\mathrm{nir}}$ and $T_{\mathrm{fir}}$ are near- and far-infrared temperatures to be defined and $C_{\mathrm{nir}}$ and $C_{\mathrm{fir}}$ are constants, determined from the conditions $C_{\mathrm{nir}} B_\lambda(T_{\mathrm{nir}}) = F_{\lambda_1}$ and $C_{\mathrm{fir}} B_{\lambda_2}(T_{\mathrm{fir}}) = F_{\lambda_2}$. The wavelengths $\lambda_1$ and $\lambda_2^1$ are the first and last wavelengths for which near-infrared and IRAS photometry is available, so $\lambda_2$ equals 60 or 100 μm depending upon whether or not a reliable 100 μm flux is available. This implies that optical measurements were not considered. First, optical photometry is in general available only for the optical carbon stars and not for the infrared carbon stars. Secondly, due to the intrinsic variability of many AGB stars, especially in the optical, and an uncertain correction for interstellar extinction these measurements yield unreliable estimates of the spectral energy distribution. Because the contribution of the second integral on the right-hand side to the total flux is on an average about 20% for group II, 6% for group III and even less for group IV stars, our approximation of using a blackbody in the optical region, even if it is accurate to only a factor of two, will introduce an error in $BC_{12}$ of less than about 0.10 magnitudes for group II stars and less for stars in the other groups. The third integral on the right-hand side is evaluated by connecting all observed spectral points by straight lines and integrating under the curve. This is accurate to within 10–20%. The two wavelengths $\lambda_{\min}$ and $\lambda_{\max}$ are determined in such a way that the first and last integral may be neglected, contributing less than 1% to the total flux. To be specific, $\lambda_{\min}$ was determined from

$$\int_0^{\lambda_{\min}} B_\lambda \mathrm{d}\lambda < B_{\lambda_{\min}} \lambda_{\min} = 0.01 \frac{\sigma T_{\mathrm{nir}}^4}{\pi}. \quad (4)$$

Solving this equation yields

$$\lambda_{\min} = \frac{1110}{T_{\mathrm{nir}}}\ \mu\mathrm{m}. \quad (5)$$

The second integral on the right-hand side of Eq. (3) is, of course, evaluated only when $\lambda_{\min}$ is smaller than $\lambda_1$. If $\lambda_{\max}$ is large so that $x = hc/kT\lambda_{\max} < 1$, the exponential in the Planck function can be approximated as $\exp(x) = 1 + x + x^2/2 + \ldots$. Because $1 + x < \exp(x)$ the following inequality holds:

$$\int_{\lambda_{\max}}^\infty B_\lambda \mathrm{d}\lambda < \int_{\lambda_{\max}}^\infty \frac{2ckT}{\lambda^4}\mathrm{d}\lambda = \frac{2ckT}{3\lambda_{\max}^3} = 0.01\frac{\sigma T_{\mathrm{fir}}^4}{\pi}. \quad (6)$$

Solving this equation yields

$$\lambda_{\max} = \frac{36000}{T_{\mathrm{fir}}}\ \mu\mathrm{m}. \quad (7)$$

If $\lambda_{\max}$ was smaller than $\lambda_2$, the observed flux was nevertheless integrated to $\lambda_2$. The far-infrared temperature $T_{\mathrm{fir}}$ is determined as the lowest colour temperature as derived from the values of $C_{21}$, $C_{32}$ and $C_{43}$, when available, using Table VI.C.6 in the "Explanatory Supplement". The near-infrared temperature $T_{\mathrm{nir}}$ is derived by fitting a blackbody of temperature $T_{\mathrm{nir}}$ to the J, H, K, L, M flux densities.

Near- and mid-infrared photometry was available for a large number of sources in our sample. For most of the group II and some group III stars photometry was available from Noguchi et al. (1981). For some group III and many group IV objects photometry was taken from Epchtein et al. (1987, 1990). Other measurements were directly obtained from or through references found in the "Catalog of Infrared Observations" (Gezari et al. 1987). From the available near-infrared magnitudes flux densities $F_\lambda$(W/m$^2$/μm) were calculated using as much as possible the calibration constants of the photometric system in which the magnitudes were given. If no near-infrared photometry was available for a star, a typical value was assigned to $T_{\mathrm{nir}}$: 2500 K in the case of a group II star, 1400 K for group III, 850 K for group IV and 700 K for group V. These values are averages of the values obtained from the sources in each group for which the near-infrared temperature could be determined from a fit to the near-infrared colours. This procedure was necessary for 20 stars in our total sample of 110 stars.

The flux densities were corrected for interstellar extinction using a visual extinction of

$$A_V = 0.18\frac{(1 - \mathrm{e}^{-11.1 D \sin b})}{\sin b} \quad (8)$$

(Milne & Aller 1980), where $D$ is the distance in kpc and $b$ is the absolute value of the galactic latitude. Extinction at other wavelengths ($0.125 < \lambda < 3.4$ μm) was calculated from Cardelli et al. (1988) using $R_V = 3.1$. Extinction at $\lambda > 3.5$ μm was neglected. The values of $A_V$ range from about 0.2 for nearby stars to about 2.5 for distant stars close to the galactic plane. The interstellar extinction correction has only a small effect on the derived near-infrared temperatures.

The distances were iteratively determined from Eqs. (3) and (8) using $M_{\mathrm{bol}} = -4.9$ ($L = 7050 L_\odot$) for all carbon stars, based on the mean value observed in the LMC (Frogel et al. 1980). In Sect. 7 we will discuss the effect of choosing a different luminosity for each group separately.

The derived values of the near-infrared temperatures, the bolometric correction, the total flux and the distance as well as the galactic longitude and latitude are listed for all stars in Table 2. The stars for which we had to assume a near-infrared temperature have a semicolon (:) in the column of $T_{\mathrm{nir}}$ as well as in the column listing the bolometric corrections. The bolometric corrections (for the stars with a reliable value for $BC_{12}$) are plotted against $C_{21}$ in Fig. 2. The values obtained and characteristic values for the different groups were already presented in Sect. 3.

We conclude this section with a comparison between the bolometric corrections derived in this work with the ones given by van der Veen & Breukers (1989) for their smaller ($\sim$30) sample of carbon stars. In Fig. 2 we have also plotted the fit presented by van der Veen & Breukers for carbon stars (the dashed line) valid in the range $-1.4 < C_{21} < -0.4$. It can be seen that their bolometric corrections are too low for the higher values of $C_{21}$. Also it is clear that their fit does not represent group II objects well. A convenient fit to our data which may be used for groups III, IV and V is:

$$BC_{12} = 8.2 - 3.37\ 10^{-2}\,\mathrm{e}^{-3.37 C_{21}} \quad (9)$$

This is the solid line in Fig. 2. For group II objects we suggest to use the constant value of 4.15 (see also Table 6). Equation (9)

**Table 2.** Derived parameters for the stars in the IBCSS

| IRAS name | $l$ | $b$ | $T_{nir}$ (K) | $F$ ($10^{-10}$) (W/m$^2$) | $BC_{12}$ | $D$ (kpc) |
|---|---|---|---|---|---|---|
| *Group II* | | | | | | |
| 01247−3248 | 250.15 | −80.6 | 2700 | 34.0 | 3.95 | 0.26 |
| 03374+6229 | 141.15 | 6.0 | 2340 | 10.6 | 4.73 | 0.46 |
| 05028+0106 | 199.02 | −22.8 | 2540 | 21.2 | 4.37 | 0.33 |
| 05426+2040 | 187.05 | −4.3 | 2610 | 15.0 | 4.55 | 0.39 |
| 06331+3839 | 176.52 | 13.8 | 2560 | 30.0 | 4.28 | 0.27 |
| 10329−3918 | 276.21 | 16.8 | 2260 | 28.4 | 3.93 | 0.28 |
| 10350−1307 | 259.94 | 38.1 | 2730 | 37.0 | 3.97 | 0.25 |
| 12427+4542 | 126.50 | 71.7 | 2460 | 36.2 | 4.19 | 0.25 |
| 12544+6615 | 122.13 | 51.1 | 2580 | 16.4 | 4.08 | 0.37 |
| 15094−6953 | 314.60 | −10.5 | 2490 | 32.8 | 4.01 | 0.26 |
| 17314−3255 | 355.35 | −0.1 | 2500(:) | 23.9 | 4.13(:) | 0.31 |
| 19017−0545 | 29.34 | −5.5 | 2280 | 17.3 | 4.33 | 0.36 |
| 20180+4744 | 84.20 | 6.6 | 2290 | 4.82 | 5.51 | 0.68 |
| 21412+3747 | 86.91 | −11.4 | 2300 | 10.8 | 4.51 | 0.58 |
| 23430+0312 | 92.95 | −55.5 | 2670 | 32.6 | 3.72 | 0.26 |
| *Group III* | | | | | | |
| 01105+6241 | 125.46 | 0.2 | 1570 | 2.06 | 6.62 | 1.05 |
| 02270−2619 | 215.81 | −68.2 | 1230 | 4.62 | 6.39 | 0.70 |
| 03229+4721 | 148.17 | −7.6 | 1360 | 7.47 | 6.76 | 0.55 |
| 03488+3943 | 156.60 | −10.9 | 1380 | 1.91 | 6.70 | 1.09 |
| 04573−1452 | 214.31 | −31.3 | 1920 | 12.1 | 5.79 | 0.43 |
| 05238+3406 | 173.49 | −0.5 | 1770 | 4.05 | 6.00 | 0.75 |
| 06226−0905 | 218.12 | −10.0 | 1410 | 2.02 | 6.56 | 1.06 |
| 06529+0626 | 207.73 | 3.8 | 1810 | 3.72 | 5.71 | 0.78 |
| 07065−7256 | 284.19 | −24.8 | 1360 | 5.33 | 6.07 | 0.65 |
| 07373−4021 | 254.02 | −9.0 | 1550 | 5.35 | 5.96 | 0.65 |
| 08088−3243 | 250.73 | 0.4 | 1400(:) | 2.12 | 7.72(:) | 1.03 |
| 10131+3049 | 197.72 | 55.9 | 1010 | 19.3 | 7.71 | 0.34 |
| 10492−2059 | 268.97 | 33.6 | 1870 | 28.9 | 6.12 | 0.28 |
| 11186−5528 | 290.37 | 4.9 | 1630 | 0.59 | 8.26 | 1.95 |
| 11318−7256 | 297.33 | −11.2 | 1400(:) | 8.63 | 5.21(:) | 0.34 |
| 12298−5754 | 300.44 | 4.6 | 980 | 1.84 | 6.95 | 1.11 |
| 12394−4338 | 301.16 | 18.9 | 1200 | 1.59 | 7.18 | 1.19 |
| 12447+0425 | 300.26 | 67.0 | 1840 | 4.24 | 6.38 | 0.73 |
| 15148−4940 | 325.76 | 6.4 | 970 | 3.26 | 6.52 | 0.83 |
| 15194−5115 | 325.53 | 4.7 | 1040 | 7.11 | 7.84 | 0.56 |
| 15477+3943 | 63.26 | 51.2 | 1945 | 3.39 | 5.77 | 0.82 |
| 16545−4214 | 343.54 | 0.3 | 1400(:) | 13.1 | 5.80(:) | 0.42 |
| 17389−5742 | 334.72 | −14.2 | 1400(:) | 3.80 | 5.81(:) | 0.77 |
| 17446−7809 | 315.43 | −23.6 | 1130 | 4.45 | 7.13 | 0.71 |
| 17556+5813 | 86.74 | 29.9 | 1530 | 3.26 | 6.54 | 0.83 |
| 18040−0941 | 19.18 | 5.4 | 1270 | 2.73 | 6.88 | 0.91 |
| 18041−3317 | 358.57 | −6.2 | 1130 | 1.33 | 6.83 | 1.30 |
| 18397+1738 | 47.78 | 10.0 | 1320 | 5.54 | 7.14 | 0.64 |
| 18398−0220 | 29.87 | 1.0 | 940 | 3.81 | 7.60 | 0.77 |
| 19008+0726 | 40.95 | 0.8 | 1200 | 5.62 | 6.92 | 0.63 |
| 19175−0807 | 28.99 | −10.0 | 2630 | 6.14 | 6.70 | 0.61 |
| 19321+2757 | 62.56 | 4.0 | 1320 | 4.51 | 6.88 | 0.71 |
| 20396+4757 | 86.52 | 3.8 | 1340 | 13.0 | 6.38 | 0.42 |
| 21032−0024 | 49.58 | −29.6 | 730 | 6.07 | 6.39 | 0.61 |
| 21035+5136 | 91.80 | 3.2 | 1280 | 2.70 | 7.11 | 0.92 |

**Table 2** (continued)

| IRAS name | $l$ | $b$ | $T_{nir}$ (K) | $F$ ($10^{-10}$) (W/m$^2$) | $BC_{12}$ | $D$ (kpc) |
|---|---|---|---|---|---|---|
| 21320+3850 | 86.27 | −9.4 | 1520 | 6.17 | 6.17 | 0.61 |
| 21358+7823 | 113.83 | 19.4 | 1330 | 13.6 | 5.72 | 0.41 |
| 21440+7324 | 110.64 | 15.4 | 1650 | 6.75 | 5.33 | 0.58 |
| 23320+4316 | 108.45 | −17.2 | 1130 | 6.33 | 7.66 | 0.60 |
| *Group IV* | | | | | | |
| 00247+6922 | 120.85 | 6.9 | 1520 | 1.96 | 7.70 | 1.07 |
| 02152+2822 | 145.04 | −30.5 | 850(:) | 1.75 | 7.00(:) | 1.14 |
| 02293+5748 | 136.06 | −2.2 | 520 | 0.63 | 8.50 | 1.89 |
| 03186+7016 | 135.07 | 11.2 | 2530 | 1.19 | 7.45 | 1.38 |
| 03448+4432 | 152.94 | −7.6 | 850(:) | 1.56 | 7.13(:) | 1.20 |
| 04307+6210 | 145.97 | 9.9 | 1230 | 3.96 | 6.63 | 0.76 |
| 05405+3240 | 176.59 | 1.6 | 950 | 1.56 | 7.56 | 1.20 |
| 06012+0726 | 200.82 | −7.1 | 614 | 1.51 | 8.13 | 1.22 |
| 06291+4319 | 171.64 | 15.1 | 1370 | 0.90 | 7.37 | 1.58 |
| 06342+0328 | 208.22 | −1.7 | 840 | 1.66 | 7.73 | 1.17 |
| 07098−2012 | 233.30 | −4.8 | 1000 | 1.71 | 7.49 | 1.15 |
| 07217−1246 | 228.07 | 1.2 | 950 | 0.77 | 7.82 | 1.71 |
| 07454−7112 | 283.38 | −21.5 | 860 | 8.10 | 6.90 | 0.53 |
| 08074−3615 | 253.53 | −1.8 | 850(:) | 2.17 | 7.01(:) | 1.02 |
| 08340−3357 | 254.78 | 3.9 | 790 | 0.76 | 7.76 | 1.73 |
| 09116−2439 | 252.74 | 16.2 | 560 | 2.37 | 8.47 | 0.98 |
| 09452+1330 | 221.45 | 45.0 | 914 | 196 | 8.16 | 0.11 |
| 09513−5324 | 278.33 | 0.5 | 730 | 1.63 | 7.24 | 1.18 |
| 09521−7508 | 292.25 | −16.4 | 920 | 3.81 | 7.13 | 0.77 |
| 11145−6534 | 293.43 | −4.7 | 760 | 1.24 | 7.68 | 1.35 |
| 12540−6845 | 303.46 | −6.2 | 880 | 3.03 | 7.07 | 0.86 |
| 13477−6532 | 309.03 | −3.6 | 850(:) | 2.99 | 6.49(:) | 0.87 |
| 13482−6716 | 308.69 | −5.3 | 840 | 1.60 | 6.80 | 1.19 |
| 14484−6152 | 316.59 | −2.4 | 720 | 2.91 | 8.01 | 0.88 |
| 15082−4808 | 325.64 | 8.3 | 720 | 3.87 | 8.02 | 0.76 |
| 16079−4812 | 333.59 | 2.3 | 680 | 0.77 | 8.06 | 1.71 |
| 17049−2440 | 358.85 | 9.3 | 780 | 3.62 | 8.12 | 0.79 |
| 17079−6554 | 325.52 | −15.4 | 810 | 1.20 | 7.47 | 1.37 |
| 17079−3243 | 352.70 | 4.0 | 850(:) | 2.15 | 7.03(:) | 1.03 |
| 17446−4048 | 350.06 | −6.6 | 850(:) | 3.00 | 7.03(:) | 0.87 |
| 18036−2344 | 6.87 | −1.4 | 850(:) | 0.94 | 7.63(:) | 1.55 |
| 18119−2244 | 8.67 | −2.6 | 890 | 0.77 | 7.59 | 1.71 |
| 18156−0653 | 23.03 | 4.2 | 1370 | 1.80 | 6.63 | 1.12 |
| 18194−2708 | 5.59 | −6.2 | 830 | 3.04 | 8.03 | 0.86 |
| 18239−0655 | 23.97 | 2.3 | 740 | 1.56 | 7.64 | 1.20 |
| 18240+2326 | 51.51 | 15.8 | 640 | 2.71 | 8.34 | 0.91 |
| 18248−0839 | 22.54 | 1.3 | 770 | 1.04 | 7.78 | 1.48 |
| 18276−4717 | 347.75 | −16.4 | 970 | 1.99 | 7.35 | 1.07 |
| 18475+0926 | 41.22 | 4.7 | 900 | 1.30 | 7.86 | 1.32 |
| 19594+4047 | 76.52 | 5.6 | 670 | 2.31 | 7.77 | 1.21 |
| 20072+3116 | 69.33 | −0.9 | 1090 | 2.02 | 7.07 | 1.06 |
| 20311+4222 | 81.17 | 1.6 | 830 | 0.89 | 7.59 | 1.59 |
| 20435+3825 | 79.49 | −2.7 | 850(:) | 1.78 | 7.03(:) | 1.13 |
| 20570+2714 | 72.57 | −12.0 | 910 | 3.12 | 7.12 | 0.85 |
| 21373+4540 | 91.62 | −5.0 | 850(:) | 1.45 | 7.02(:) | 1.25 |

**Table 2** (continued)

| IRAS name | $l$ | $b$ | $T_{nir}$ (K) | $F$ ($10^{-10}$) (W/m$^2$) | $BC_{12}$ | $D$ (kpc) |
|---|---|---|---|---|---|---|
| 21489+5301 | 97.81 | −0.6 | 850(:) | 1.57 | 7.00(:) | 1.20 |
| 22241+6005 | 105.84 | 2.4 | 820 | 1.99 | 7.25 | 1.07 |
| 23257+1038 | 92.22 | −46.9 | 990 | 1.24 | 7.80 | 1.35 |
| *Group V* | | | | | | |
| 01144+6658 | 125.49 | 4.5 | 590 | 0.69 | 8.26 | 1.81 |
| 04395+3601 | 166.44 | −6.5 | 840 | 3.01 | 8.02 | 0.87 |
| 08171−2134 | 242.45 | 8.1 | 700(:) | 1.24 | 7.37(:) | 1.35 |
| 17534−3030 | 359.87 | −2.9 | 700(:) | 1.48 | 7.74(:) | 1.24 |
| 19075+0921 | 43.32 | 0.2 | 700(:) | 0.59 | 8.35(:) | 1.96 |
| 21318+5631 | 98.22 | 3.7 | 700(:) | 2.25 | 7.58(:) | 1.00 |
| 23166+1655 | 93.50 | −40.3 | 850 | 3.02 | 8.35 | 0.86 |
| 15471−5644 | 325.64 | −2.2 | 700(:) | 1.63 | 7.35(:) | 1.18 |

*Note*: A semicolon (:) in the column of the near-IR temperatures indicates an assumed value for $T_{nir}$ (see text). The corresponding value of $BC_{12}$ is therefore also uncertain.

**Table 3.** Association of the IBCSS with other catalogues

| IRAS name | AFGL | IRC | GCCCS | Name | HD |
|---|---|---|---|---|---|
| *Group II* | | | | | |
| 01247−3248 | 215 | −30015 | 68 | R Scl | 8879 |
| 03374+6229 | 505 | 60124 | 154 | U Cam | 22611 |
| 05028+0106 | 683 | 00066 | 284 | W Ori | 32736 |
| 05426+2040 | 5168 | 20121 | 393 | Y Tau | 38307 |
| 06331+3839 | 966 | 40158 | 537 | UU Aur | 46687 |
| 10329−3918 | | | 1706 | U Ant | |
| 10350−1307 | 1427 | −10242 | 1714 | U Hya | 92055 |
| 12427+4542 | 1576 | 50219 | 2030 | Y CVn | 110914 |
| 12544+6615 | 1588 | 70116 | 2047 | RY Dra | 112559 |
| 15094−6953 | 4985S | | 2219 | X Tra | |
| 17314−3255 | 5354 | | (1) | | |
| 19017−0545 | 2314 | −10486 | 2695 | V Aql | 177336 |
| 20180+4744 | 2556 | 50324 | 2894 | U Cyg | 193680 |
| 21412+3747 | 2798 | 40491 | 3063 | RV Cyg | 206750 |
| 23430+0312 | 3142 | 00532 | 3202 | TX Psc | 223075 |
| *Group III* | | | | | |
| 01105+6241 | 177 | 60041 | 59 | NSV00438 | |
| 02270−2619 | 337 | −30021 | 103 | R For | |
| 03229+4721 | 489 | 50096 | 142 | V384 Per | |
| 03488+3943 | 527 | 40070 | | V414 Per | |
| 04573−1452 | 667 | −10080 | 276 | R Lep | 31996 |
| 05238+3406 | 748 | 30114 | 336 | S Aur | 35556 |
| 06226−0905 | 933 | −10122 | | V636 Mon | |
| 06529+0626 | 1038 | 10144 | 615 | CL Mon | |
| 07065−7256 | 4070 | | 689 | R Vol | |
| 07373−4021 | | | 849 | | |
| 08088−3243 | 1235 | | 1081 | | |
| 10131+3049 | 1403 | 30219 | 1641 | RW Lmi | |
| 10492−2059 | 1439 | −20218 | 1766 | V Hya | |
| 11186−5528 | 4130 | | 1839 | | |
| 11318−7256 | 4133 | | 1882 | | |

**Table 3** (continued)

| IRAS name | AFGL | IRC | GCCCS | Name | HD |
|---|---|---|---|---|---|
| 12298−5754 | 4151 | | 2012 | | |
| 12394−4338 | | | 2025 | NSV05868 | |
| 12447+0425 | 1579 | 00224 | 2032 | RU Vir | 111166 |
| 15148−4940 | | | 2232 | | |
| 15194−5115 | | | | | |
| 15477+3943 | 5311 | 40273 | 2293 | V CrB | 141826 |
| 16545−4214 | | | 2380 | | |
| 17389−5742 | | | 2470 | V Pav | 160435 |
| 17446−7809 | | | 2476 | | |
| 17556+5813 | 2040 | 60255 | 2512 | T Dra | |
| 18040−0941 | 2067 | −10396 | | FX Ser | |
| 18041−3317 | | | (2) | | |
| 18397+1738 | 2232 | 20370 | | NSV11125 | |
| 18398−0220 | 2233 | 00365 | 2642 | NSV11233 | |
| 19008+0726 | 2310 | 10401 | 2694 | NSV11689 | |
| 19175−0807 | 2368 | −10502 | | NSV11913 | |
| 19321+2757 | 2417 | 30374 | | V1129 Cyg | |
| 20396+4757 | 2632 | 50338 | 2923 | V Cyg | |
| 21032−0024 | 2702 | 00499 | 2968 | RV Aqr | |
| 21035+5136 | 2704 | 50357 | 2976 | V1549 Cyg | |
| 21320+3850 | 2781 | 40485 | 3041 | V1426 Cyg | |
| 21358+7823 | 2758 | 80048 | 3055 | S Cep | 206362 |
| 21440+7324 | 2805 | 70177 | 3070 | PQ Cep | |
| 23320+4316 | 3116 | 40540 | | NSV14623 | |
| *Group IV* | | | | | |
| 00247+6922 | 67 | | | | |
| 02152+2822 | | | | | |
| 02293+5748 | 341 | | | | |
| 03186+7016 | 482 | | | | |
| 03448+4432 | 5102 | | | | |
| 04307+6210 | 595 | | | | |
| 05405+3240 | 809 | | | V370 Aur | |
| 06012+0726 | 865 | | | | |
| 06291+4319 | 954 | | | | |
| 06342+0328 | 971 | | | | |
| 07098−2012 | 1085 | | (3) | | |
| 07217−1246 | 5230 | | (4) | | |
| 07454−7112 | 4078 | | | | |
| 08074−3615 | | | | | |
| 08340−3357 | 5251 | | | | |
| 09116−2439 | 5254 | | | | |
| 09452+1330 | 1381 | 10216 | | CW Leo | |
| 09513−5324 | | | | | |
| 09521−7508 | 4098 | | | | |
| 11145−6534 | | | | | |
| 12540−6845 | 4159 | | | | |
| 13477−6532 | 4183 | | | | |
| 13482−6716 | 4918S | | | | |
| 14484−6152 | 4202 | | (5) | | |
| 15082−4808 | 4211 | | | | |

**Table 3** (continued)

| IRAS name | AFGL | IRC | GCCCS | Name | HD |
|---|---|---|---|---|---|
| 16079−4812 | | | | | |
| 17049−2440 | 1922 | | | | |
| 17079−6554 | | | | | |
| 17079−3243 | | | | | |
| 17446−4048 | | | | | |
| 18036−2344 | 5440 | | | V449 Cyg | |
| 18119−2244 | 2096 | | | | |
| 18156−0653 | 2118 | | | | |
| 18194−2708 | 2135 | | | | |
| 18239−0655 | 2154 | | | | |
| 18240+2326 | 2155 | | | | |
| 18248−0839 | | | | | |
| 18276−4747 | | | | | |
| 18475+0926 | 2259 | | | | |
| 19594+4047 | 2494 | | | | |
| 20072+3116 | 2513 | | | | |
| 20311+4222 | 2604 | | | | |
| 20435+3825 | | | | | |
| 20570+2714 | 2826 | | | | |
| 21373+4540 | | | | | |
| 21489+5301 | | | | | |
| 22241+6005 | 2901 | | | | |
| 23257+1038 | 3099 | | | | |
| *Group V* | | | | | |
| 01144+6658 | 190 | | | | |
| 04395+3601 | 618 | | | V353 Aur | |
| 08171−2134 | 5250 | | | V2003 Sgr | |
| 17534−3030 | 5416 | | | | |
| 19075+0921 | 2333 | | | | |
| 21318+5631 | 5625S | | | | |
| 23166+1655 | 3068 | | | | |
| 15471−5644 | | | | | |

(1) Listed in Fuenmayor (1981) as star 245
(2) Listed in Fuenmayor (1981) as star 272
(3) Listed in MacConnell (1988) as star 145
(4) Listed in MacConnell (1988) as star 192
(5) Listed in MacConnell (1988) as star 462

was derived excluding the uncertain bolometric corrections (:) in Table 2.

## 5. Mass loss rates

For carbon stars two different methods of determining mass loss rates are available: based on infrared data and based on CO data.

In general, accurate mass loss rates can be determined from a comparison of the observed spectral energy distribution with the results of detailed radiative transfer calculations, modelling the emission of a star surrounded by a dust shell. Such modelling is outside the scope of this paper. We also could have used formulae like those derived by Herman et al. (1986) and Jura (1987) based on the 60 μm flux, or the one presented by van der Veen (1989) and van der Veen & Rugers (1989) based on the $C_{21}$ colour. The advantage of these formulae is that they can be applied to *all* stars, the disadvantage is the large error in individual determinations, due to uncertain input physics and input parameters. The formulae of Herman et al. and Jura e.g. assume a certain emissivity law ($Q_\lambda \sim 1/\lambda$) and a certain grain size distribution. Furthermore, they require the knowledge of the dust-to-gas ratio and the opacity of the dust at 60 μm. The formulae of van der Veen and van der Veen & Rugers do not depend on input physics – they are true fit formulae – but the authors note that the correlation they

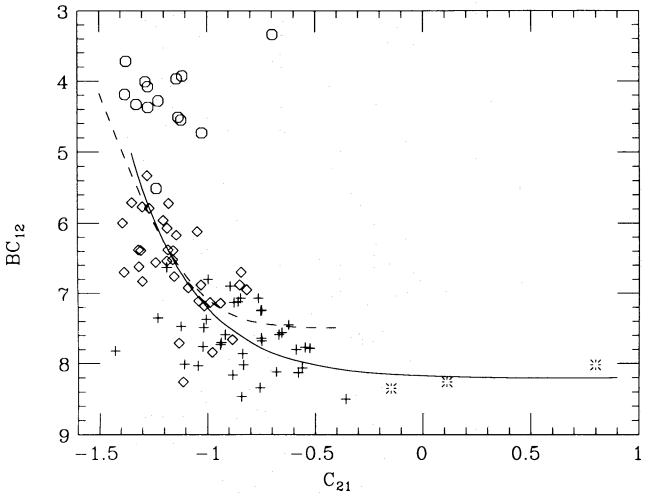


**Fig. 2.** The bolometric correction $BC_{12}$ plotted against $C_{21}$ colour. Indicated are group II (○), group III (◇), group IV (+) and group V (*). Only stars with a reliable bolometric correction are plotted. The dashed line is the fit of van der Veen & Breukers (1989) derived for a much smaller sample of carbon stars. The solid line is the fit we prefer for groups III, IV and V; see Eq. (9)

find is much worse for carbon stars than for oxygen-rich stars. Besides, their relation is valid only in the range $-1.4 \leq C_{21} \leq -0.4$, whereas our sample contains stars outside this region.

For these reasons we have used the other alternative and determined the mass loss rates of our stars from $^{12}$CO line emission measurements. These were available for most of our stars but biased towards group II. For group II stars measurements were available for 13 out of 15 stars, for group III for 28 out of 39, for group IV for 29 out of 48 and for group V for 6 out of 8 stars.

The general formula to derive the mass loss rate from CO emission in the case of an optically thick line is given by Knapp & Morris (1985) and Olofsson et al. (1990):

$$\frac{\dot{M}}{D^2} = \left(1 + \frac{4N_{\rm He}}{N_{\rm H}}\right) \frac{T_{\rm mb} V_{\rm e}^2}{A(B,J) f_{\rm CO}^{0.85}}, \tag{10}$$

where $T_{\rm mb}$ is the main-beam brightness temperature, $V_{\rm e}$ the terminal velocity, $f_{\rm CO}$ the CO abundance relative to $H_2$ and $A(B,J)$ depends on the size of the telescope and the observed transition. For an unresolved envelope $A(B,J)$ is given by (van der Veen & Olofsson 1990)

$$A(B,J) = 2\ 10^{19} B^{-2} s(J) \tag{11}$$

if in Eq. (10) $V_{\rm e}$ is given in km/s, $D$ the distance to the source in pc and $\dot{M}$ in $M_\odot$/yr. $B$ is the full beam width at half power of the telescope in arcseconds and $s(J)$ is a correction factor. For the $J=1$–0 transition $s(1)$ equals 1 and for the $J=2$–1 transition $s(2)$ equals 0.6 (van der Veen & Olofsson 1990). There are two important restrictions to Eqs. (10) and (11) which need further attention. First of all Eq. (10) is, strictly speaking, valid only in the case of an optically thick line. Knapp & Morris (1985) also presented a formula in the case of an optically thin CO line, but this formula is now known to be incorrect due to an incorrect photodissociation model used (van der Veen & Olofsson 1990). Van der Veen & Rugers (1990) showed, however, using the detailed fits of Knapp & Morris for optically thin CO lines and Eq. (10) that the error in using Eq. (10) in the case of optically thin CO lines is less than a factor of 2. So Eq. (10) can also be used rather well in the case of an optically thin CO line. The second restriction is that Eq. (11) is valid only in the case of an unresolved CO envelope. Van der Veen & Olofsson do not present a similar formula in the case of a resolved envelope. To decide whether a source is unresolved in a certain transition by a certain telescope we proceed as follows. For both optically thin and thick lines the region which contributes significantly to the CO ($J=1$–0) emission is given by (see the discussion in van der Veen & Olofsson)

$$R_{1-0} = 5\ 10^{16} \left(\frac{\dot{M}}{10^{-6} M_\odot/{\rm yr}}\right)^{0.6} \left(\frac{f_{\rm CO}}{4\ 10^{-4}}\right)^{0.5} \left(\frac{15\ {\rm km/s}}{V_{\rm e}}\right)^{0.5} {\rm cm}. \tag{12}$$

For higher transitions this region will be smaller. An estimate for the $J=2$–1 transition is given by $R_{2-1} = 0.2 R_{1-0}$ (van der Veen & Olofsson). A source is thus unresolved if

$$\frac{2R_{J\rightarrow J-1}}{D} \ll B(J \rightarrow J-1). \tag{13}$$

To determine the most reliable mass loss rates we proceeded in the following way. From various sources the following data were collected: $T_{\rm mb}$, $V_{\rm e}$, $B$ and the observed transition. In some cases the value of the terminal velocity was considered unreliable by the authors. In these cases the values of $V_{\rm e}$ found from HCN measurements were used, if available. Using Eq. (10), $\dot{M}/D^2$ was calculated ($N_{\rm He}/N_{\rm H}=0.1$ and $f_{\rm CO}=8\ 10^{-4}$ were used throughout) and then $\dot{M}$ was found based on the distances derived in Sect. 3. With the derived mass loss rate Eq. (12) can be evaluated and condition (13) verified. The results are presented in Table 4 where all observations of our stars are collected in order of decreasing telescope beamwidth. Papers listing only antenna temperatures or integrated intensities instead of main-beam temperatures were not included in Table 4.

A similar approach was taken by van der Veen & Rugers (1989) who collected data for all sources detected in the CO ($J=1$–0) and CO($J=2$–1) line and listed in the IRAS PSC. Their list contains 133 sources, 53 of which are carbon-rich. Our list gives information on 76 carbon stars of our sample. The total number of carbon stars observed in any of the CO lines already exceeds 100 by now (Olofsson 1989). Van der Veen & Rugers calculated mass loss rates using an equation similar to Eq. (10) but they did not correct for the helium abundance and used a different value for $s(2)$. They did not take condition (13) into account in deriving the mass loss rates.

From the data in Table 4 we can deduce the importance of taking condition (13) into account when deriving the most reliable mass loss rates, instead of e.g. averaging the available data. From the data for which multiple measurements are available (e.g. IRAS 01247−3248, 10131+3049, 10492−2059, 20396+4757, 23320+4316) it can be seen that *Eq. (10) systematically gives higher mass loss rates for unresolved sources.* This in itself is not surprising since a telescope which resolves an envelope samples less CO emission. Using the mass loss rates of the stars for which multiple measurements are available we derive that the difference between the values of $\dot{M}$ based on the most resolved and the most unresolved case amounts to a factor of 1.4–1.9. One may argue that this is a small factor compared to the error made

**Table 4.** CO data for stars in the IBCSS

| IRAS name | $M/D^2$ ($M_\odot$/yr/kpc$^2$) | $V_e$ (km/s) | CO transition | Source size(″) | Beam width(″) | Ref. | Remarks |
|---|---|---|---|---|---|---|---|
| *Group II* | | | | | | | |
| 01247−3248 | 3.0 (−5) | 17.5 | $J=1$–0 | 51 | 100 | 1 | Average $V_e$ used |
| | 2.7 (−5) | 17.6 | 1–0 | 48 | 65 | 1 | |
| | 1.7 (−5) | 17.5 | 1–0 | 37 | 52 | 5 | |
| | 1.8 (−5) | 17.5 | 1–0 | 38 | 40 | 9 | |
| 03374+6229 | 4.9 (−6) | 22.0 | 1–0 | 17 | 46 | 3 | |
| | 2.5 (−6) | 18.0 | 1–0 | 13 | 33 | 7 | |
| 05028+0106 | 9.6 (−7) | 11.8 | 1–0 | 8.3 | 33 | 7 | |
| | 9.8 (−7) | 10.2 | 2–1 | 1.8 | 29 | 2 | |
| 05426+2040 | 1.1 (−6) | 15.9 | 1–0 | 8.1 | 46 | 3 | |
| | 1.2 (−6) | 10.7 | 1–0 | 10 | 40 | 9 | |
| | 2.0 (−6) | 14.9 | 1–0 | 12 | 33 | 7 | |
| 06331+3839 | 2.0 (−6) | 11.4 | 1–0 | 13 | 33 | 7 | |
| | 3.7 (−6) | 11.5 | 2–1 | 3.6 | 29 | 2 | |
| | 1.1 (−6) | 12.4 | 2–1 | 1.7 | 24 | 3 | |
| 10329−3918 | 1.1 (−5) | 21.2 | 1–0 | 26 | 40 | 9 | |
| 10350−1307 | 1.1 (−6) | 7.9 | 1–0 | 10 | 40 | 9 | |
| | 4.3 (−6) | 10.7 | 2–1 | 4.1 | 29 | 2 | |
| 12427+4542 | 1.1 (−6) | 7.9 | 1–0 | 10 | 100 | 1 | |
| | 9.0 (−7) | 9.0 | 1–0 | 8.7 | 33 | 7 | |
| | 6.3 (−7) | 6.3 | 2–1 | 1.7 | 29 | 2 | |
| | 5.8 (−7) | 7.3 | 2–1 | 1.5 | 25 | 4 | |
| 12544+6615 | 5.2 (−7) | 10.0 | 1–0 | 6.4 | 33 | 7 | |
| 15094−6953 | 8.1 (−7) | 9.2 | 1–0 | 8.1 | 40 | 9 | |
| 19017−0545 | 7.7 (−7) | 8.0 | 1–0 | 9.0 | 40 | 9 | |
| | 5.7(−7) | 8.2 | 1–0 | 7.4 | 33 | 7 | |
| | 8.9 (−7) | 10.4 | 2–1 | 1.7 | 27 | 8 | |
| 21412+3747 | 1.6 (−6) | 14.7 | 1–0 | 11 | 33 | 7 | |
| 23430+0312 | 1.5 (−6) | 10.6 | 1–0 | 11 | 52 | 5 | |
| | 1.6 (−6) | 12.1 | 1–0 | 11 | 40 | 9 | |
| | 1.3 (−6) | 11.8 | 1–0 | 9.5 | 33 | 7 | |
| *Group III* | | | | | | | |
| 01105+6241 | 2.0 (−6) | 23.3 | 2–1 | 2.3 | 27 | 8 | |
| 02270−2619 | 3.1 (−6) | 20.0 | 1–0 | 15 | 40 | 9 | |
| | 5.3 (−6) | 16.8 | 2–1 | 4.5 | 29 | 2 | |
| 03229+4721 | 1.8 (−5) | 16.8 | 1–0 | 45 | 100 | 1 | |
| | 1.5 (−5) | 16.8 | 1–0 | 40 | 65 | 1 | |
| 04573−1452 | 1.1 (−5) | 20.5 | 1–0 | 29 | 100 | 1 | |
| | 3.8 (−6) | 18.6 | 1–0 | 16 | 40 | 9 | |
| | 8.8 (−6) | 19.0 | 2–1 | 5.2 | 29 | 2 | Average $V_e$ used |
| 05238+3406 | 1.4 (−6) | 16.5 | 1–0 | 10 | 46 | 3 | |
| 06226−0905 | 1.3 (−5) | 25.8 | 2–1 | 6.8 | 27 | 8 | |
| 06529+0626 | 4.0 (−6) | 23.9 | 1–0 | 16 | 55 | 8 | |
| | 2.8 (−6) | 27.4 | 1–0 | 12 | 40 | 9 | |
| | 4.3 (−6) | 27.0 | 2–1 | 3.2 | 27 | 8 | |
| 07065−7256 | 2.9 (−6) | 19.3 | 1–0 | 15 | 40 | 9 | |
| 08088−3243 | 1.3 (−5) | 20.7 | 2–1 | 7.5 | 29 | 2 | |
| 10131+3049 | 6.3 (−5) | 16.9 | 1–0 | 86 | 100 | 1 | |
| | 3.5 (−5) | 17.1 | 1–0 | 60 | 65 | 1 | |
| | 4.4 (−5) | 17.5 | 1–0 | 68 | 55 | 8 | |
| | 4.1 (−5) | 16.3 | 1–0 | 68 | 52 | 5 | |
| | 4.3 (−5) | 16.5 | 1–0 | 69 | 46 | 3 | |
| | 4.5 (−5) | 17.4 | 2–1 | 14 | 29 | 2 | |
| | 4.4 (−5) | 17.4 | 2–1 | 14 | 27 | 8 | |
| | 4.4 (−5) | 17.3 | 2–1 | 14 | 27 | 8 | |

**Table 4** (continued)

| IRAS name | $M/D^2$ ($M_\odot$/yr/kpc$^2$) | $V_e$ (km/s) | CO transition | Source size(″) | Beam width(″) | Ref. | Remarks |
|---|---|---|---|---|---|---|---|
| | 4.0 (−5) | 17.8 | 2–1 | 13 | 24 | 3 | |
| | 3.9 (−6) | 17.1 | 1–0 | 16 | 21 | 11 | |
| 10492−2059 | 1.3 (−5) | 14.0 | 1–0 | 35 | 100 | 1 | There is also a |
| | 1.3 (−5) | 14.0 | 1–0 | 35 | 65 | 1 | broad component |
| | 1.1 (−5) | 14.0 | 1–0 | 32 | 55 | 8 | at $V_e \approx 22$ km/s |
| | 9.2 (−6) | 14.2 | 1–0 | 29 | 52 | 5 | but the dominant |
| | 1.7 (−5) | 15.8 | 1–0 | 39 | 40 | 9 | emission is at |
| | 2.9 (−5) | 14.0 | 2–1 | 11 | 27 | 8 | $V_e = 14$ km/s |
| 12447+0425 | 6.0 (−6) | 16.9 | 1–0 | 25 | 100 | 1 | |
| 15194−5115 | 5.4 (−5) | 26.0 | 1–0 | 70 | 44 | 16 | |
| | 1.6 (−4) | 23.3 | 2–1 | 28 | 32 | 11 | |
| 15477+3943 | 3.0 (−7) | 6.5 | 1–0 | 6.6 | 46 | 3 | |
| 17556+5813 | 4.1 (−6) | 14.0 | 1–0 | 22 | 100 | 1 | |
| 18040−0941 | 5.3 (−6) | 29.7 | 2–1 | 3.6 | 27 | 8 | |
| 18397+1738 | 2.3 (−5) | 15.6 | 1–0 | 56 | 100 | 1 | |
| | 2.3 (−5) | 14.3 | 1–0 | 57 | 65 | 1 | |
| | 1.5 (−5) | 15.6 | 1–0 | 45 | 52 | 5 | |
| | 1.4 (−5) | 14.0 | 1–0 | 44 | 46 | 3 | |
| | 8.0 (−6) | 11.9 | 2–1 | 11 | 25 | 4 | |
| 18398−0220 | 2.2 (−5) | 34.5 | 1–0 | 36 | 46 | 3 | |
| 19008+0726 | 1.3 (−5) | 28.0 | 1–0 | 29 | 46 | 3 | $V_e$ from HCN |
| 19175−0807 | 1.3 (−5) | 30.5 | 1–0 | 28 | 100 | 13 | |
| | 9.7 (−6) | 22.5 | 2–1 | 5.5 | 29 | 2 | |
| 19321+2757 | 2.0 (−5) | 24.4 | 2–1 | 8.3 | 29 | 2 | |
| 20396+4757 | 1.9 (−5) | 13.1 | 1–0 | 50 | 100 | 1 | |
| | 1.4 (−5) | 11.8 | 1–0 | 44 | 65 | 1 | |
| | 1.0 (−5) | 11.7 | 1–0 | 36 | 46 | 3 | |
| | 1.1 (−5) | 11.8 | 2–1 | 7.6 | 29 | 2 | |
| | 1.7 (−5) | 11.7 | 2–1 | 9.8 | 27 | 8 | |
| | 9.0 (−6) | 11.9 | 2–1 | 6.7 | 27 | 8 | |
| 21032−0024 | 7.3 (−6) | 16.4 | 1–0 | 27 | 100 | 1 | |
| | 4.0 (−6) | 16.1 | 1–0 | 19 | 40 | 9 | |
| 21035+5136 | 1.9 (−6) | 11.4 | 2–1 | 3.1 | 27 | 8 | |
| 21320+3850 | 7.3 (−6) | 14.9 | 1–0 | 28 | 100 | 1 | |
| | 1.2 (−5) | 14.9 | 1–0 | 38 | 65 | 1 | |
| 21358+7823 | 1.1 (−5) | 22.4 | 2–1 | 5.5 | 29 | 2 | |
| | 1.1 (−5) | 27.0 | 1–0 | 25 | 22 | 14 | $V_e$ from profile |
| 21440+7324 | 4.5 (−6) | 21.7 | 1–0 | 17 | 46 | 3 | |
| 23320+4316 | 3.0 (−5) | 14.7 | 1–0 | 66 | 100 | 1 | |
| | 2.5 (−5) | 14.5 | 1–0 | 60 | 65 | 1 | |
| | 2.1 (−5) | 13.8 | 1–0 | 55 | 46 | 3 | |
| | 1.6 (−5) | 14.8 | 2–1 | 9.1 | 27 | 8 | |
| *Group IV* | | | | | | | |
| 02152+2822 | 4.2 (−7) | 8.9 | 1–0 | 7.5 | 55 | 8 | |
| | 5.4 (−7) | 9.5 | 2–1 | 1.7 | 29 | 2 | |
| 02293+5748 | 4.6 (−6) | 14.2 | 2–1 | 5.5 | 24 | 3 | |
| 03186+7016 | 8.4 (−6) | 16.0 | 1–0 | 35 | 100 | 1 | |
| 03448+4432 | 1.8 (−6) | 13.3 | 2–1 | 3.0 | 29 | 2 | |
| 04307+6210 | 1.5 (−5) | 20.4 | 1–0 | 39 | 100 | 1 | |
| | 5.8 (−6) | 14.5 | 1–0 | 26 | 52 | 5 | |
| 05405+3240 | 1.5 (−5) | 30.0 | 1–0 | 35 | 100 | 13 | |
| | 1.9 (−5) | 26.0 | 2–1 | 8.7 | 29 | 2 | |
| 06012+0726 | 1.1 (−5) | 17.5 | 1–0 | 39 | 100 | 1 | |
| | 1.1 (−5) | 16.4 | 1–0 | 40 | 42 | 15 | |
| | 3.7 (−5) | 15.1 | 2–1 | 17 | 30 | 17 | |

**Table 4** (continued)

| IRAS name | $M/D^2$ ($M_\odot$/yr/kpc$^2$) | $V_e$ (km/s) | CO transition | Source size(″) | Beam width(″) | Ref. | Remarks |
|---|---|---|---|---|---|---|---|
| 06291+4319 | 1.7 (−6) | 21.4 | 1–0 | 12 | 46 | 3 | |
| 06342+0328 | 2.6 (−6) | 9.0 | 2–1 | 4.5 | 29 | 2 | |
| 07098−2012 | 4.8 (−6) | 23.8 | 2–1 | 4.0 | 29 | 2 | |
| 07217−1246 | 1.1 (−6) | 24.9 | 1–0 | 8.6 | 21 | 6 | |
| 08074−3615 | 4.9 (−6) | 17.3 | 1–0 | 23 | 52 | 5 | |
| 09116−2439 | 9.6 (−6) | 13.4 | 1–0 | 39 | 52 | 5 | |
| | 1.4 (−5) | 12.8 | 2–1 | 9.9 | 29 | 2 | |
| 09452+1330 | 3.5 (−4) | 15.2 | 1–0 | 203 | 100 | 1 | |
| | 2.2 (−4) | 15.3 | 1–0 | 153 | 65 | 1 | |
| | 1.8 (−4) | 15.6 | 1–0 | 134 | 55 | 8 | |
| | 1.9 (−4) | 15.9 | 1–0 | 138 | 52 | 5 | |
| | 1.5 (−4) | 15.0 | 1–0 | 123 | 46 | 3 | |
| | 1.3 (−4) | 16.0 | 1–0 | 109 | 40 | 9 | |
| | 1.9 (−4) | 14.7 | 2–1 | 29 | 29 | 2 | |
| | 1.7 (−4) | 15.3 | 2–1 | 26 | 27 | 8 | |
| | 1.7 (−4) | 15.1 | 2–1 | 26 | 27 | 8 | |
| | 7.2 (−5) | 14.6 | 2–1 | 16 | 24 | 3 | |
| | 6.2 (−5) | 15.3 | 2–1 | 72 | 21 | 11 | |
| 15082−4808 | 4.1 (−5) | 20.5 | 2–1 | 14 | 32 | 11 | |
| 17049−2440 | 3.2 (−5) | 20.7 | 1–0 | 62 | 100 | 13 | |
| | 8.4 (−6) | 16.6 | 2–1 | 6.1 | 24 | 3 | |
| 17079−3243 | 5.0 (−6) | 25.6 | 2–1 | 3.7 | 27 | 8 | |
| 18194−2708 | 2.7 (−5) | 23.0 | 1–0 | 53 | 100 | 13 | |
| 18239−0655 | 1.2 (−5) | 27.0 | 1–0 | 32 | 46 | 3 | |
| 18240+2326 | 1.2 (−5) | 15.1 | 1–0 | 41 | 100 | 1 | |
| | 9.8 (−6) | 15.1 | 1–0 | 36 | 65 | 1 | |
| 18248−0839 | 6.2 (−7) | 16.1 | 1–0 | 7.4 | 21 | 6 | |
| 18475+0926 | 5.1 (−6) | 21.8 | 1–0 | 22 | 46 | 3 | |
| 19594+4047 | 1.1 (−5) | 22.5 | 1–0 | 33 | 100 | 13 | |
| | 1.7 (−5) | 20.0 | 2–1 | 8.9 | 29 | 2 | |
| 20435+3825 | 6.8 (−7) | 20.7 | 1–0 | 6.3 | 21 | 6 | |
| 20570+2714 | 8.7 (−6) | 23.5 | 2–1 | 5.4 | 29 | 2 | |
| 21373+4540 | 1.3 (−6) | 14.7 | 1–0 | 11 | 21 | 6 | |
| 21489+5301 | 2.7 (−5) | 22.3 | 2–1 | 12 | 29 | 2 | |
| | 1.2 (−5) | 20.7 | 1–0 | 37 | 21 | 6 | |
| 22241+6005 | 1.5 (−5) | 34.2 | 1–0 | 32 | 46 | 3 | |
| 23257+1038 | 4.9 (−6) | 10.1 | 1–0 | 32 | 100 | 1 | |
| *Group V* | | | | | | | |
| 01144+6658 | 8.9 (−6) | 19.7 | 2–1 | 6.9 | 29 | 2 | |
| 04395+3601 | 6.0 (−5) | 21.5 | 1–0 | 90 | 100 | 1 | |
| | 2.7 (−5) | 18.0 | 2–1 | 12 | 31 | 12 | |
| | 1.5 (−5) | 18.5 | 1–0 | 42 | 21 | 10 | |
| | 2.0 (−5) | 18.5 | 2–1 | 10 | 13 | 10 | |
| 08171−2134 | 3.0 (−6) | 15.8 | 1–0 | 19 | 52 | 5 | |
| | 4.4 (−6) | 16.1 | 2–1 | 4.7 | 29 | 2 | |
| 17534−3030 | 2.0 (−5) | 31.8 | 1–0 | 41 | 52 | 5 | |
| 21318+5631 | 8.0 (−6) | 15.6 | 1–0 | 32 | 46 | 3 | |
| 23166+1655 | 2.3 (−5) | 14.5 | 1–0 | 61 | 100 | 1 | |
| | 2.2 (−5) | 13.4 | 1–0 | 62 | 65 | 1 | |
| | 1.5 (−5) | 12.2 | 1–0 | 52 | 46 | 3 | |

*References*: (1) Knapp & Morris (1985); (2) Zuckerman & Dyck (1986a); (3) Zuckerman et al. (1986); (4) Wannier & Sahai (1986); (5) Zuckerman & Dyck (1986b); (6) Nguyen-Q-Rieu et al. (1987); (7) Olofsson et al. (1987); (8) Zuckerman & Dyck (1987); (9) Olofsson et al. (1988); (10) Bachiller et al. (1988); (11) Knapp et al. (1989); (12) Huggins & Healey (1990); (13) Knapp (1986); (14) Bujarrabal et al. (1989); (15) Sopka et al. (1989); (16) Booth et al. (1989); (17) Wannier et al. (1990)

in applying Eq. (10), which is based on a fit to uncertain model calculations of CO emission. However, since the differences in mass loss rate between the resolved and the unresolved case are systematic rather than random we feel that our procedure of taking this into account is to be preferred.

The "best-estimate" mass loss rates are collected in Table 5. These were selected from Table 4 using the entry with the lowest value of "source size/beam width", that is, the most unresolved value. Information on the degree of resolution of the envelope was also included in Table 5. The following criteria were used. For values of the "source size/beam width" of $<0.1$, between 0.1 and 0.5, between 0.5 and 1 or $>1$, the envelope is called unresolved, partially unresolved, partially resolved or resolved, respectively. It can be seen that in most cases the mass loss rates

**Table 5.** Derived mass loss rates

| IRAS name | $\dot{M}$ ($M_\odot$/yr) | Status envelope | IRAS name | $\dot{M}$ ($M_\odot$/yr) | Status envelope |
|---|---|---|---|---|---|
| *Group II* | | | | | |
| 01247−3248 | 2.03 (−6) | PR | 12427+4542 | 3.63 (−8) | U |
| 03374+6229 | 1.04 (−6) | PU | 12544+6615 | 7.12 (−8) | PU |
| 05028+0106 | 1.07 (−7) | U | 15094−6953 | 5.48 (−8) | PU |
| 05426+2040 | 1.67 (−7) | PU | 19017−0545 | 1.15 (−7) | U |
| 06331+3839 | 8.02 (−8) | U | 21412+3747 | 3.39 (−7) | PU |
| 10329−3918 | 8.62 (−7) | P | 23430+0312 | 1.01 (−7) | PU |
| 10350−1307 | 2.69 (−7) | PU | | | |
| *Group III* | | | | | |
| 01105+6241 | 2.20 (−6) | U | 18040−0941 | 4.39 (−9) | PU |
| 02270−2619 | 2.60 (−6) | PU | 18397+1738 | 3.30 (−6) | PU |
| 03229+4721 | 5.45 (−6) | PU | 18398−0220 | 1.30 (−5) | PR |
| 04573−1452 | 1.63 (−6) | PU | 19008+0726 | 5.16 (−6) | PR |
| 05238+3406 | 7.88 (−7) | PU | 19175−0807 | 3.61 (−6) | PU |
| 06226−0905 | 1.46 (−5) | PU | 19321+2757 | 1.01 (−5) | PU |
| 06529+0626 | 2.62 (−6) | PU | 20396+4757 | 1.94 (−6) | PU |
| 07065−7256 | 1.23 (−6) | PU | 21032−0024 | 2.72 (−6) | PU |
| 08088−3243 | 1.38 (−5) | PU | 21035+5136 | 1.61 (−6) | PU |
| 10131+3049 | 5.20 (−6) | PU | 21320+3850 | 2.72 (−6) | PU |
| 10492−2059 | 1.02 (−6) | PU | 21358+7823 | 1.85 (−6) | PU |
| 12447+0425 | 3.20 (−6) | PU | 21440+7324 | 1.51 (−6) | PU |
| 15194−5115 | 4.95 (−5) | PR | 23320+4316 | 5.76 (−6) | PU |
| 15477+3943 | 1.98 (−7) | PU | | | |
| 17556+5813 | 2.82 (−6) | PU | | | |
| *Group IV* | | | | | |
| 02152+2822 | 7.02 (−7) | U | 17049−2440 | 5.24 (−6) | PU |
| 02293+5748 | 1.64 (−5) | PU | 17079−3243 | 3.70 (−6) | PU |
| 03186+7016 | 1.60 (−5) | PU | 18194−2708 | 2.00 (−5) | PR |
| 03448+4432 | 2.59 (−6) | PU | 18239−0655 | 1.73 (−5) | PR |
| 04307+6210 | 8.66 (−6) | PU | 18240+2326 | 9.94 (−6) | PU |
| 05405+3240 | 2.74 (−5) | PU | 18248−0839 | 1.36 (−6) | PU |
| 06012+0726 | 1.67 (−5) | PU | 18475+0926 | 8.89 (−6) | PU |
| 06291+4319 | 4.24 (−6) | PU | 19595+4047 | 1.67 (−5) | PU |
| 06342+0328 | 3.56 (−6) | PU | 20435+3825 | 6.14 (−7) | PU |
| 07098−2012 | 6.35 (−6) | PU | 20570+2714 | 6.29 (−6) | PU |
| 07217−1246 | 3.22 (−6) | PU | 21373+4540 | 1.43 (−6) | PR |
| 08074−3615 | 5.06 (−6) | PU | 21489+5301 | 3.84 (−5) | PU |
| 09116−2439 | 1.34 (−5) | PU | 22241+6005 | 1.72 (−5) | PR |
| 09452+1330 | 2.06 (−6) | PU | 23257+1038 | 8.93 (−6) | PU |
| 15082−4808 | 2.37 (−5) | PU | | | |
| *Group V* | | | | | |
| 01144+6658 | 2.92 (−5) | PU | 17534−3030 | 3.08 (−5) | PR |
| 04395+3601 | 2.04 (−5) | PU | 21318+5631 | 8.00 (−6) | PR |
| 08171−2134 | 8.02 (−6) | PU | 23166+1655 | 1.70 (−5) | PR |

*Note*: U: unresolved; PU: partially unresolved; PR: partially resolved. See text for explanation.

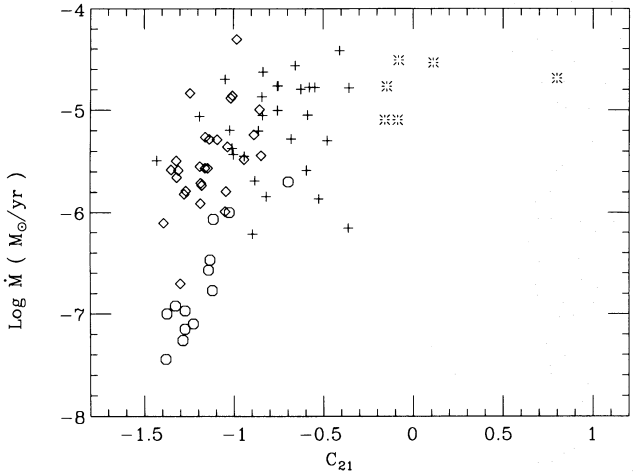


**Fig. 3.** The mass loss rates of group II (○), group III (◇) group IV (+) and group V (∗) plotted against $C_{21}$ colour

have been derived from measurements where the envelope was at most partially resolved, so it is expected that the derived mass loss rates are not systematically underestimated.

Since it is expected that the mass loss rate increases from group II to group V (see Sect. 2), we have plotted in Fig. 3 the mass loss rate versus $C_{21}$ for all groups. Although there is a large scatter (which is shown below to be at least partly due to the range in expansion velocities for fixed $C_{21}$), it is obvious that $\dot{M}$ increases with $C_{21}$, especially within groups II and III and then seems to level off at a value of $\dot{M} \approx 3.2\ 10^{-5} M_\odot$/yr for groups IV and V. This corresponds to a ratio of momentum flux in the wind ($\dot{M} V_e$) to that of the stellar luminosity ($L/c$) of $\tau = \dot{M} V_e c/L = 4.5$ if one assumes $V_e = 20$ km/s. The average value of $\tau$ for group III is about 0.4. Linear least-square fits were made to the data in Fig. 3 to obtain

$$\log \dot{M} = -6.736 + 1.550\ C_{21} + 1.687 \log V_e \quad \text{(group II)}, \tag{14}$$

$$\log \dot{M} = -6.104 + 1.324\ C_{21} + 1.677 \log V_e \quad \text{(group III)}. \tag{15}$$

For groups IV and V it is not very useful to derive such relations because of the scatter. These groups are best represented by an average value (see Table 6). Equations (14) and (15) give mass loss rates accurate to within a factor of 1.3 and 1.7, respectively.

From the data in Table 4 we derive average expansion velocities of 12.7, 19.4, 17.3 and 19.4 km/s for groups II, III, IV and V and we conclude that the average expansion velocities for groups III, IV and V are about the same at $V_e \approx 19$ km/s. Only group II stars have a significantly lower expansion velocity, possibly related to the building up of the circumstellar envelope after the transition from oxygen- to carbon-rich and the start of the carbon-rich mass loss phase.

Van der Veen & Rugers (1989) also presented a fit to the mass loss rate. Their result for carbon stars is

$$\dot{M} = 3\ 10^{-5} \left(\frac{L}{10^4 L_\odot}\right) \left(\frac{V_e}{15\ \text{km/s}}\right)^{2.2} \left(\frac{S_{25}}{S_{12}}\right)^{2.6}. \tag{16}$$

Using our value of $L = 7050 L_\odot$ this can be recast into

$$\log \dot{M} = -7.261 + 1.041\ C_{21} + 2.2 \log V_e. \tag{17}$$

Because their fit is valid only for $C_{21} \leq -0.4$, it can best be compared to Eq. (15) for group III stars. For a typical star with $C_{21} = -1.0$ and $V_e = 20$ km/s our value is about 50% higher. At $C_{21} = -0.4$ the difference is a factor of 2.3. We expect our results to be higher because we took the correction for the helium abundance [see Eq. (10)] into account and we explicitly searched for measurements which did not resolve the envelope and which on an average result in higher mass loss rates compared to e.g. averaging the available mass loss rates in the case of multiple measurements. The main difference between Eq. (15) and Eq. (17) lies in the dependence on the expansion velocity. Our dependence

**Table 6.** Space densities and timescales for the IBCSS

| Group | | II | III | IV | V | Total |
|---|---|---|---|---|---|---|
| Number | | 15 | 39 | 48 | 7–8 | 109–110 |
| $BC_{12}$ | | $4.25 \pm 0.51$ | $6.65 \pm 0.67$ | $7.61 \pm 0.48$ | $8.21 \pm 0.17$ | |
| $\log \dot{M}(M_\odot/\text{yr})$ | | $-6.72 \pm 0.54$ | $-5.49 \pm 0.46$ | $-5.17 \pm 0.47$ | $-4.78 \pm 0.26$ | |
| $(m_{12} - M_{12})_{\text{lim}}$ | | 7.78 | 10.18 | 11.14 | 11.74 | |
| $d_{\text{lim}}$(pc) | | 360 | 1090 | 1690 | 2230 | |
| $H$(pc) | | $290 \pm 100$ | $260 \pm 40$ | $155 \pm 20$ | $195 \pm 20$ | 190 |
| Effective volume[1] | $H = 150$ pc | 0.093 | 1.08 | 2.65 | 4.63 | |
| (kpc$^3$) | $H = 300$ pc | 0.13 | 1.94 | 5.05 | 9.01 | |
| Number density | $H = 150$ pc | 162 | 36 | 18 | 1.5–1.7 | 218 |
| (kpc$^{-3}$) | $H = 300$ pc | 116 | 20 | 9.5 | 0.8–0.9 | 146 |
| Surface density | $H = 150$ pc | 48 | 11 | 5.4 | ~0.5 | 65 |
| (kpc$^{-2}$) | $H = 300$ pc | 69 | 12 | 5.7 | ~0.5 | 87 |
| Time (yr) | $H = 150$ pc | 20000 | 4440 | 2220 | 185–210 | 26860 |
| | $H = 300$ pc | 20000 | 3450 | 1640 | 140–150 | 25240 |
| $\Delta M\ (M_\odot)$[2] | $H = 150$ pc | 0.004 | 0.014 | 0.015 | 0.003 | 0.037 |
| | $H = 300$ pc | 0.004 | 0.011 | 0.011 | 0.002 | 0.029 |

[1] Calculated from Eq. (19)
[2] $\Delta M = \text{Time} * \dot{M}$

is less steep. An increase in the expansion velocity by 10 km/s to 30 km/s will result in an increase in the mass loss rate by a factor of 1.9 in our case and by a factor of 2.4 in the case of van der Veen & Rugers.

## 6. An evolutionary sequence for carbon stars

In this section our flux-limited sample of carbon stars will be transformed into a volume-complete sample. Local number densities for the different groups will be derived and evolutionary timescales and the amount of matter lost in the different evolutionary phases will be calculated. All relevant data are gathered in Table 6. Preliminary results were presented at the Montpellier conference by de Jong (1990).

Average bolometric corrections were calculated for each group. Uncertain values of $BC_{12}$, listed in Table 2 with a semicolon (:) were not used. The bolometric correction increases steadily from 4.2 for group III to 8.2 for group V as discussed in Sect. 3. Averages per group of $\log \dot{M}$ were calculated from the data in Table 5. As could already be seen in Fig. 4, the mass loss rate steadily increases from group II to group V, confirming the idea that a carbon star evolves from left (near the blackbody line; group III) to right ($C_{21}>0$; group V) in the $C_{21}$ vs. $C_{32}$ colour–colour diagram (see Fig. 1) after the mass loss has resumed (group II).

The limiting distance to which our sample can be observed is calculated from $m_{12}-M_{12}=5\log d-5$, where $m_{12}=-2.5\log(100/28.3)=-1.37$, is the limiting 12 μm magnitude for our sample of carbon stars with $S_{12}>100$ Jy. The absolute magnitude $M_{12}=M_{\rm bol}-BC_{12}$ [see Eq. (1)] can be calculated from our assumed value of $M_{\rm bol}=-4.9$ and the average value of the bolometric correction $BC_{12}$ for each group.

To transform the flux-limited sample into a volume-complete sample we have to take into account the fact that the carbon stars are concentrated towards the galactic plane. Since our sample is confined to the solar neighbourhood ($D<2$ kpc) and Thronson et al. (1987) and Jura et al. (1989) found no gradient of carbon stars along the Galactocentric axis on a scale of at least 4 kpc, we assume that the number density of carbon stars varies like

$$\rho=\rho_0\,\mathrm{e}^{-|z|/H} \tag{18}$$

in the solar neighbourhood, where $z$ is the distance to the galactic plane and $H$ is the scale height. We find that the number of stars within a distance $R$ equals

$$\begin{aligned} N(R)&=\int\rho\,\mathrm{d}V=2\int_0^R\int_0^{\sqrt{R^2-z^2}}\int_0^{2\pi}\rho_0\mathrm{e}^{-z/H}\,r\,\mathrm{d}\phi\,\mathrm{d}r\,\mathrm{d}z\\ &=2\pi\rho_0\int_0^R\mathrm{e}^{-z/H}(R^2-z^2)\,\mathrm{d}z\\ &=2\pi\rho_0 H^3\left[2\mathrm{e}^{-R/H}\left(\frac{R}{H}+1\right)+\left(\frac{R}{H}\right)^2-2\right] \end{aligned}$$

or, equivalently,

$$N(R)=2\pi\rho_0 R^2 H\left\{1-2\left(\frac{H}{R}\right)^2+2\mathrm{e}^{-R/H}\left[\frac{H}{R}+\left(\frac{H}{R}\right)^2\right]\right\}. \tag{19}$$

In the limiting case of $R\ll H$ Eq. (19) gives $N(R)=(4/3)\pi R^3\rho_0$, as expected. If $R\gg H$, Eq. (19) gives $N(R)=(\pi R^2)(2H)\rho_0$, the volume of a cylinder with height $2H$ times the density. Because both $N(R)$ and $R$ are known, the local number density $\rho_0$ can be calculated for each group if $H$ is known.

The scale height $H$ is related to the average value $z_{\rm mean}\equiv|z|=|D\sin(b)|$ through

$$\begin{aligned} z_{\rm mean}&=\frac{\int z\rho\,\mathrm{d}V}{\int\rho\,\mathrm{d}V}\\ &=H\,\frac{1-6(H/R)^2+2\mathrm{e}^{-R/H}[1+3(H/R)+3(H/R)^2]}{1-2(H/R)^2+2\mathrm{e}^{-R/H}[H/R+(H/R)^2]}. \end{aligned} \tag{20}$$

When $R\gg H$ we simply have $|z|=H$; for $R\ll H$ we have $|z|=(3/8)R$. The derived values of $H$ are listed in Table 6. The errors quoted for $H$ are based on a hypothetical 10% error in $|z|$. The value of $H$ quoted for the whole sample is a weighted mean of the values for the different groups. We find values between 150 and 300 pc with a mean close to 200 pc. This compares well to the value of $H=200$ pc found by Claussen et al. (1987) and Jura & Kleinmann (1989). In the calculations presented below we consider $H=150$ and 300 pc. The effective volume $(N(R)/\rho_0)$ for $H=150$ and 300 pc are listed in Table 6. The local space density $\rho_0$ is given in the next entry in Table 6. In the last column we give the total galactic carbon star number density. For groups III, IV and V $\rho_0$ scales with $H$ because $R\gg H$ but since the space density for group II is not so sensitive to $H(R\approx H)$ and is by far the largest contributor to the total, the total number density of carbon stars does not depend too strongly on the exact value of $H$. The total number density of carbon stars in the solar neighbourhood is 150–220 kpc$^{-3}$ depending upon the scale height.

The time spent in each phase is proportional to the numbers of stars in that phase. The number densities can therefore be transformed into timescales when the absolute timescale of one of the groups is known. The evolution of group II stars has been investigated by Willems & de Jong (1988) and Chan & Kwok (1988). They modelled the transition from oxygen- to carbon-rich stars using a radiative transfer model. The position of the carbon stars with a 60 μm excess (group II) in the colour–colour diagram could be reproduced quite well. The timescale derived for the group II phase range from about 10 000 years (Willems & de Jong) to about 50 000 years (Chan & Kwok). The best estimate for the timescale of the group II phase can be made by comparing the position of our group II and III stars with the model tracks of Chan & Kwok (their Fig. 8). We find that carbon stars spend about 20 000 years as a group II star. This number is uncertain to a factor of 2. Using this timescale for group II the times spent by a carbon star in the other phases can be calculated from their number relative to the number in group II. The total lifetime of the carbon star phase is about 26 000 years. The time spent as a group III, IV or V star is only about 25% of the total lifetime.

Using the time spent in each phase and the average mass loss during that phase we can calculate the total mass lost in each phase. The best estimate of the total mass lost during the carbon star phase is about $0.04M_\odot$. The uncertainty in this number is a factor of 3 due to the error in the average mass loss rates, especially of group IV. If the average mass loss rates would be increased by their respective one-sigma values, the total mass lost would increase to $0.105M_\odot$. Although group III and IV represent only 25% of the total lifetime, they account for 80% of the total mass lost by the carbon star.

Our results imply that the stellar mass of the average star when it is transformed into a carbon star is already quite close to the white dwarf mass. If we assume an average white dwarf mass

of $0.65M_\odot$, the mass of a newly formed carbon star would be $0.69M_\odot$. An upper limit of $0.87M_\odot$ can be derived by taking the high values of the mass loss rates (average values in Table 6 increased by $1\sigma$) and revising the lifetime of group II upwards by its uncertainty of a factor of 2. In calculating this quantity we did not take into account the possibility of a "superwind", or a sudden ejection of a part of the remaining envelope. Because a superwind phase would take place at the end of the carbon life, i.e. while a star is in group V, and there is no star with an extremely high mass loss rate in our sample, we conclude that such a superwind phase, if it exists, lasts less than approximately 20 years. If during this short period the mass loss rate would be $10^{-3}M_\odot$/yr the extra mass lost in this superwind would be $0.02M_\odot$. Although this is almost equal to the mass lost in the preceding 26 000 years, it does not significantly alter the estimates given above for the average mass of a newly formed carbon star. A superwind phase would increase the most probable average mass of a newly formed carbon star to $0.71M_\odot$ and make it certainly less than $0.89M_\odot$.

Such a low mass ($0.69$–$0.85M_\odot$) at the onset of the carbon star phase may seem low but is in fair agreement with current AGB evolution models. The models of Boothroyd & Sackmann (1988b; BS), which include mass loss using Reimers law, predict a stellar mass at the first thermal pulse (TP) of $0.81M_\odot$ for a $M_{\rm initial}=1M_\odot$, $Z=0.001$ star, and $0.90M_\odot$ for a $M_{\rm initial}=1.2M_\odot$, $Z=0.02$ star. In calculating these numbers we have reduced the mass loss rates of BS by a factor of 1.5 because BS estimate their mass loss rates to be overestimated by this factor due to their particular choice of $\eta=0.4$ and $\alpha=1$ ($\eta$ being the coefficient in Reimers law and $\alpha$ the mixing-length parameter). If we assume a duration of the oxygen-rich TP-AGB phase of typically $10^6$ years and an average observed mass loss rate of optically visible oxygen-rich AGB stars of $=1.5\,10^{-7}M_\odot$/yr (Kleimann 1989), an average oxygen-rich star loses about $0.15M_\odot$ before turning into a carbon star. If we subtract this amount of the stellar mass at the first TP, we derive a likely average mass of a newly formed carbon star of $0.66$–$0.75M_\odot$. So, from this analysis we estimate that stars with initial masses between $0.9M_\odot$ and $1.5$–$2M_\odot$ can become carbon stars at a stellar mass of $0.69$–$0.85M_\odot$, depending upon the exact details of the mass loss process.

This result seems in conflict with recent evolutionary calculations which produce carbon stars only from stars of relative high initial mass, unless the metallicity is low and the mixing-length parameter high: e.g. $M_{\rm initial}=1.2M_\odot$ ($Z=0.001$, $\alpha=3$, Boothroyd & Sackmann 1988c) or $M_{\rm initial}=1.5M_\odot$ ($Z=0.01$, Lattanzio 1989). Our result is an indication that carbon stars are formed from lower mass stars, i.e. at lower luminosity than predicted by evolutionary calculations. This seems confirmed by a comparison of theoretically predicted luminosities with the observed LF of carbon stars in the Magelleanic Clouds. The low luminosity tail of the carbon star LF extends down to $M_{\rm bol}\approx -3.8$ in the LMC (Frogel et al. 1980) and $M_{\rm bol}\approx -3.4$ in the SMC (Westerlund et al. 1986). Some of these low-luminosity carbon stars may be high-luminosity R-stars, which are probably not related to the third dredge-up phase. The theoretically predicted lowest carbon star luminosity (i.e. in the post-flash luminosity dip) are $M_{\rm bol}=-3.6$ ($Z=0.001$, $\alpha=3$, Boothroyd & Sackmann 1988c) and $M_{\rm bol}=-4.0$ ($Z=0.01$, Lattanzio 1989).

Our result that most carbon stars have low-mass progenitors does not imply that high-mass carbon stars do not exist, or are not present in our sample. Our sample, containing stars distributed according to the initial mass function, obviously is dominated by stars of low mass.

We finally note that kinematical studies (see e.g. Feast 1990) also indicate that the bulk of the carbon stars are of low mass ($\approx 1.6M_\odot$).

From the data in Table 6 we can derive the amount of mass returned to the interstellar medium (ISM) by carbon stars. Summing the contributions of the different groups we calculate a mass return of about $8.6\,10^{-5}M_\odot$/yr/kpc$^2$ or $\sim 0.06M_\odot$/yr for the whole Galaxy. These figures do not depend on $H$ since the main contributors to the mass return are groups III and IV. The uncertainty in both numbers is a factor of 3 due to the uncertainty in the mean mass loss rates for the different groups.

To check the influence of our assumed luminosity of $7050L_\odot$ for all stars on the results in Table 6, we have repeated the calculations adopting luminosities of 5000, 7050, 10 000 and $15\,000L_\odot$ for groups II, III, IV and V, respectively. These values would roughly apply if a carbon star lives long enough to increase its core mass significantly and thereby attain a higher luminosity.

For groups II, III, IV and V we find a limiting distance of 300, 1090, 2010 and 3250 pc and a scale height of 410, 260, 300 and 280 pc. For an assumed average scale height of 300 pc we find number densities of 188, 20, 6.6 and 0.4 kpc$^{-3}$ and a surface density of 113, 12, 4.0 and 0.3 kpc$^{-2}$. The total number and surface density are 215 kpc$^{-3}$ and 129 kpc$^{-2}$, respectively. We find that the number and surface density approximately scale with the assumed luminosity for group II. For the lifetimes we find 20 000, 2130, 700 and 40 years or a total lifetime of 22 880 years, and a mass loss of 0.0026, 0.0069, 0.0067, $0.0016M_\odot$, resulting in a total mass loss of $0.018M_\odot$. We conclude that the timescales and mass loss are not very sensitive to the assumed luminosities and that it does not affect the conclusions of this section.

## 7. Discussion

In the previous section we derived a carbon star number density in the solar neighbourhood of 220 kpc$^{-3}$ for our calculated scale height of $H=150$ pc (this number would be 150 kpc$^{-3}$ for $H=300$ pc and 185 kpc$^{-3}$ for $H=200$ pc). The surface density varies between 65 and 90 kpc$^{-2}$, depending on $H$. These values are higher than quoted by most other authors. Jura & Kleinmann (1989) studied dust-enshrouded stars within 1 kpc from the sun. To ensure the selection of dust-enshrouded stars they chose only stars with $S_{60}>10$ Jy which results in $\dot{M}>2\,10^{-6}M_\odot$/yr assuming – as Jura & Kleinmann did – the relation between mass loss rate and 60 μm flux of Jura (1987). This selection criterion effectively removes all our group II stars from their sample. Jura & Kleinmann found 63 stars, 29 of them being carbon stars. If we use their scale height of 200 pc and correct for the fact that they searched only for stars in the spatial zone observed in the TMSS, their number is equivalent to 32 dusty carbon stars per kpc$^3$. This is in good agreement with our value of $\rho_0$ for the sum of groups III, IV and V if we scale our result to $H=200$ pc. Claussen et al. (1987) derive $\log\rho_0=2.0\pm0.4$ (with $H=200$ pc). Our value for $H=200$ pc (185 kpc$^{-3}$) is within their quoted error but nevertheless higher. Part of this discrepancy is due to the fact that Claussen et al. studied only carbon stars found in the TMSS. This excludes our group IV and V stars. A second reason is that

Claussen et al. use an absolute $K$-magnitude of $-8.1$ to derive distances to all their sample stars. This overestimates the distance to stars affected by dust extinction at 2 μm, i.e. group III, IV and V stars. Therefore, the distances to the TMSS stars that are classified as group III stars by us have been overestimated and their number density underestimated by Claussen et al.

In Sect. 6 we derived a total lifetime of the carbon star phase of about 26 000 years, of which about 25% is spent as group III, IV or V stars. Our lifetime estimate disagrees with Claussen et al. (1987) who derived a carbon star lifetime of about $10^5$ years, and with Thronson et al. (1987) who derived an average lifetime of $2\,10^5$ yr. Jura & Kleinmann (1989) found a lifetime for the dust-enshrouded carbon stars of $>3\,10^4$ yr, significantly larger than our estimated lifetime of groups III, IV and V of $\sim 6000$ yr. Let us first comment on the lifetime derived by Thronson et al. Their value of lifetime of $2\,10^5$ yr is based on the idea that a particular envelope mass is lost in a certain time given a certain mass loss rate. However, their analysis is flawed because they took the wrong envelope mass by neglecting the mass lost prior to the carbon star phase.

The carbon star lifetime estimates of Claussen et al. (1987) and Jura & Kleinmann (1989) are based on the death rate of main-sequence stars. Let us repeat this analysis using our complete sample and also take into account the available data on Planetary Nebulae (PN). Using the surface densities and lifetimes in Table 6 we derive a carbon star birth rate of $2.4$–$3.4\,10^{-9}$ stars/pc$^2$/yr. This number should be compared to the death rate of possible carbon star progenitors on the main sequence (MS). From Scalo (1986) we derive a (present-day) death rate of MS stars with $0.98 < M_{MS}/M_\odot < 5.2$ of $5.8\,10^{-10}$ stars/pc$^2$/yr (assuming a constant birth rate and an age of the Galaxy $T_G = 12$ Gyr) or $8.2\,10^{-10}$ stars/pc$^2$/yr (with a decreasing birth rate and $T_G = 15$ *Gyr*). The formal error in these numbers is a factor of 1.7. These estimates are not sensitive to the choice of the maximum mass. If we had assumed $2.5\,M_\odot$ instead of $5.2\,M_\odot$ the death rate would drop from $5.8\,10^{-10}$ stars/pc$^2$/yr to $5.3\,10^{-10}$ stars/pc$^2$/yr. The lower mass limit is of more importance. Decreasing it to $0.83\,M_\odot$ increases the death rate by 30% to $7.8\,10^{-10}$ stars/pc$^2$/yr. Rana (1987), using new data not incorporated by Scalo, derived a death rate of $1.2\,10^{-9}$ stars/pc$^2$/yr assuming a constant birth rate and $T_G = 15$ Gyr.

So our value of the birth rate seems to be too large by a factor of 2–7. A direct comparison of the present-day death rate of main-sequence stars with the birth rate of carbon stars neglects the birth rate history of our Galaxy. If most present-day carbon stars are of low mass ($\sim M_\odot$), they were formed typically $10^{10}$ years ago when the birth rate was higher than at present. Therefore, the present day death rates should be considered a lower limit to the death rate of carbon star progenitors. Since the star formation rate $10^{10}$ years ago is about 2–3 times the average star formation rate over the age of the galaxy (see e.g. Vader & de Jong 1981), the death rate of main-sequence stars and the birth rate of carbon stars agree within a factor of 2. Let us consider now the immediate descendants of the carbon stars, the carbon-rich PN, to get independent information on the lifetime of the carbon star phase. From Phillips (1989) we have a current best estimate of the number density of PN of $90 \pm 6$ kpc$^{-3}$. Assuming that carbon stars indeed evolve into carbon-rich PN and the fact that about 60% of all PN are carbon-rich (Zuckerman & Allen 1986), we derive a number density of carbon-rich PN of about 54 kpc$^{-3}$. Assuming a lifetime of a PN of $2\,10^4$ yr and using our carbon star densities of Table 6, we derive a carbon star lifetime of $6$–$9\,10^4$ yr, about 2–3 times our best estimate. If not all carbon stars would evolve into carbon-rich PN, the agreement would improve. There are different ways to remove the discrepancy. Low-mass stars could terminate their evolution at such low core masses ($M_c \lesssim 0.56\,M_\odot$) that their evolution to the left in the HR diagram is so slow that they will never show up as PN. For this argument to hold, dredge-up should occur at somewhat lower core masses than is found in current stellar evolution models. Also hot bottom envelope burning (HBB) could convert $^{12}$C into $^{14}$N (and a little $^{13}$C) and thereby possibly transforming a carbon star back to an oxygen-rich star. Since HBB operates in stars initially more massive than about $3.5\,M_\odot$ (see e.g. Renzini & Voli 1981) only the more massive carbon stars would be affected by HBB. Observations of the Magellanic Clouds seem to indicate that HBB is indeed effective in some stars. In canonical models (i.e. without HBB) carbon stars should be the most luminous objects on the AGB since they are the endpoint of AGB evolution for stars with $1.9 \lesssim M_{MS}/M_\odot \lesssim 8$ (see Renzini & Voli 1981, their models without HBB). Lundgren (1988) finds that the most luminous AGB stars in the LMC are of spectral type MS and in addition there is evidence (Westerlund et al. 1990) that some of the most luminous carbon stars are enriched in $^{13}$C (J-type carbon stars). This suggests that HBB may have been operating in these stars. Recently, a PN in the SMC was discovered with a very low carbon abundance and enriched in He and N; this was explained in terms of HBB (Meatheringham et al. 1990). It seems, thus, possible that not all carbon stars evolve into carbon-rich PN. At this moment theory cannot give an estimate of the fraction of carbon stars which do not evolve into carbon-rich PN. Our observed number densities indicate that to bring our carbon star lifetime in agreement with that of the carbon-rich PN 60–70% of the carbon stars should not evolve into carbon-rich PN. This percentage is smaller for larger lifetimes of group II, smaller PN lifetimes and larger PN number densities. If we take 40 000 years as the lifetime of group II, 25–45% of the carbon stars need not evolve into carbon-rich PN.

Perhaps the estimated number density of PN is in error. If we use our lifetimes and number densities and a PN lifetime of $2\,10^4$ yr, and correct by a factor of 10/6 to allow for the fraction of carbon-rich PN relative to all PN, we find a PN number density of 220–320 kpc$^{-3}$. This is much higher than most quoted values but in fair agreement with the value of Ishida & Weinberger (1987), who, trying to construct a complete sample by looking only at nearby ($D < 0.5$ kpc) PN, found a value of 326 kpc$^{-3}$.

We conclude that the lifetime we derive for the carbon star phase agrees with the death rate of main-sequence stars within a factor of 2 and that the PN data suggests that our carbon lifetime is too low by a factor of 2–3.

Apart from the uncertainties in the death rates of main-sequence stars and PN data as discussed above, there are two other possibilities that could explain this difference. First of all our assumption that all group II stars are recently formed carbon stars and that their 60 μm excess is due to a remnant oxygen-rich shell may be wrong. Perhaps some carbon stars will experience another thermal pulse while on the AGB. This could be accompanied by a temporary drop in the mass loss rate, resulting in an expanding *carbon-rich* shell. Such stars would also make a loop in the IRAS colour–colour diagram. If many recently formed carbon stars experience more than one thermal pulse on the AGB as a carbon star, the lifetime of group II stars would have been

underestimated, as well as the total lifetime of the carbon star phase. We note that the typical interpulse period for a star with a core mass of $0.65\,M_{\odot}$ is about 45 000 years (Boothroyd & Sackman 1988a). Our assumption that most newly formed carbon star will not experience another thermal pulse on the AGB is consistent with our lifetime estimate of about 26 000 years.

We stress again (see also de Jong 1990) that the non-detection of several group II stars in OH by Zuckerman & Maddalena (1989) is *no* proof that the circumstellar envelope is not oxygen-rich at the radius where the 60 μm excess arises from. Using Eq. (9) of van der Veen & Olofsson (1990) one can calculate that the OH maser emission comes from a region typically $10^{15}$–$10^{16}$ cm from the star. However, Olofsson et al. (1990), from an analysis of CO maps of several group II stars, derive that the inner radius of the expanding shell which causes the 60 μm excess is at $>10^{17}$ cm.

Secondly, the assumed lifetime of group II stars is based on model calculations. The tracks in the IRAS colour–colour diagram calculated by Chan & Kwok (1988) depend on details such as grain properties or assumed condensation temperatures. Chan & Kwok use e.g. an optically thin radiative transfer model and consider only the expanding oxygen-rich shell while neglecting the start of the carbon-rich mass-losing phase. It is not inconceivable that models which include these effects properly would lead to a different lifetime of group II stars. Although we are planning such calculations, they are beyond the scope of this paper.

If the lifetime of group II stars is increased to 40 000 yr, the total lifetime of the carbon star phase would be about 50 000 yr and the total amount of mass lost would increase to about $0.07\,M_{\odot}$. The number and surface densities would remain unchanged.

The number of group V objects is low. Only a few carbon stars are known with very red colours ($C_{21} > -0.5$). We tentatively identified some objects as cool carbon stars, because their LRS spectra look similar to the LRS spectra of those few very red carbon stars. We note that there is at least one carbon star not observed by IRAS, which would be classified as a group V star, were it in our sample. The Egg Nebula (AFGL 2688) is carbon-rich, is featureless between 8 and 14 μm (Forrest et al. 1975) and from photometry of Forrest et al. (1975), Kleinmann et al. (1978) and Price & Murdock (1983) we estimate $S_{12} \approx 480$ Jy, $S_{25} \approx 4600$ Jy, $S_{60} \approx 2700$ Jy, $S_{100} \approx 1300$ Jy, so $C_{21} \approx 2.5$ and $C_{32} \approx -0.6$. A systematic search for very red carbon stars based on the SiC feature is not possible because the LRS spectra are almost featureless. A systematic search for very red carbon stars using near-infrared spectroscopy, CO and HCN measurements would reveal if extreme carbon stars are really as rare as suggested by this study. An increase in the number of group V objects would have some influence on the derived timescales but would have a large impact on the total mass lost in the carbon star phase because the mass loss rates of group V objects are generally high. A search for very red carbon stars might also shed some light on the peculiar distribution observed in Fig. 1. Most group V objects cluster around $C_{21} \approx 0$ and only the very young PPN AFGL 618 has a truly large value for $C_{21}$ and a value of $C_{32}$ very different from other group V objects. A systematic search for carbon stars with $C_{21} > -0.5$ would reveal the timescale in which carbon stars evolve off the AGB and the derived mass loss rates (from CO emission) would indicate if a superwind phase preceding the termination of the AGB phase is present or not. We have started an observational program to identify very red carbon stars with featureless LRS spectra.

Let us finally turn briefly to the group I stars, the stars which according to Willems & de Jong (1986) recently underwent the transition from oxygen-rich to carbon star. Although none of the group I stars made it into our sample (based on $S_{12} > 100$ Jy), we can perform a similar analysis using a lower limiting flux density. Of all group I stars (Willems & de Jong 1986), excluding C2123 (see Sect. 3.1) and C1633 (Le Bertre et al. 1990), four have $S_{12} > 27.5$ Jy. Although not all stars listed in the PSC with $S_{12} > 27.5$ Jy have a published LRS spectrum, we will assume that group I is complete down to this limiting flux density. Calculating bolometric corrections for group I stars according to Sect. 4 and proceeding as in Sect. 6 we find a volume density of group I stars of 1–2 $\mathrm{kpc}^{-3}$ depending upon the scale height and a surface density of 0.7 $\mathrm{kpc}^{-2}$. From this we derive a lifetime of group I stars of approximately 200 yr, for an assumed lifetime of 20 000 yr for group II and *assuming that all carbon stars go through this phase.* Our value compares well with the original lifetime estimates of 100–400 yr by Willems & de Jong (1986, 1988). However, it should be pointed out that there are several problems with the interpretation of group I stars as being transition objects. First of all model calculations of Chan & Kwok (1988) indicate that the silicate feature in an expanding shell can only be seen for at most 100 years. This difference in the lifetimes of a factor of 2 is probably not too significant, given all uncertainties. In addition, they point out that the silicate feature in group I stars is stronger than their models predict. This could be due to the opacity function Chan & Kwok adopted or point to the formation of very small grains at higher than equilibrium temperatures (Slijkhuis 1990).

A second point which *must* be addressed when explaining these stars is the fact that all are enriched in $^{13}$C. This was the original assumption of Willems & de Jong (1986) based on only 2 of their 9 stars but it has been confirmed recently that indeed all group I stars are J-type (Lloyd Evans 1990; Lambert et al. 1990). What does this imply?

Two different kinds of $^{13}$C-enriched stars are known observationally: the J-type carbon stars which, generally, are the most luminous carbon stars on the AGB (at least in the clouds) and the so-called R-stars which are of low luminosity ($M_{\mathrm{bol}} \approx -1$) and are possibly related to the helium core flash (see e.g. Parthasarathy 1991).

If we discard the binary hypothesis (Little-Marenin 1986) and the S-star hypothesis (Skinner et al. 1990) and assume that group I stars are indeed in transition from an oxygen-rich to a $^{13}$C-rich carbon star, they must be either massive ($M_{\mathrm{MS}} \gtrsim 3.5\,M_{\odot}$) to allow for HBB to enrich the star in $^{13}$C or of low mass ($M_{\mathrm{MS}} \lesssim 2M_{\odot}$) to allow the star to undergo the helium core flash. In either case the lifetime of 200 years derived above is, of course, no longer valid.

We suggest that a search for s-process elements in all group I stars should be undertaken. If they show s-process elements, group I stars are associated with the AGB and not related to the helium core flash.

*Acknowledgements.* It is a pleasure to thank Cecile Loup for providing us with a preliminary version of her list of CO observations before publication. We thank the referee, T. Le Bertre, for his swift response and helpful comments. The research of MG is supported under grant 782-373-030 by the Netherlands Foundation for Astronomical Research (ASTRON), which receives its fund from the Netherlands Organisation for Scientific Research (NWO).

**References**


Aaronson M., Blanco V.M., Cook K.H., Schechter P.L., 1989, ApJS 70, 637

Aaronson M., Blanco V.M., Cook K.H., Olszewski E.W., Schechter P.L., 1989, ApJS 73, 841

Alknis A., Alksne Z., Ozolina V., 1977, Investigations of the Sun and Red stars, ed. A. Balklavs Riga, Zinatve: Vol. 6, 55

Alknis A., Alksne Z., Ozolina V., Eglitas I., 1976, Investigations of the Sun and Red stars, ed. A. Balklavs, Zinatve Riga, Vol. 5, 15

Alknis A., Alksne Z., Ozolina V., Platais I., 1978, Investigations of the Sun and Red stars, ed. A. Balklavs, Zinatve Riga, Vol. 8, 5

Alknis A., Alksne Z., Ozolina V., Platais I., 1988, Nauchn. Inf. 65, 162

Alksne Z., Ozolina V., 1972, Astron. Tsirk. 738, 7

Alksne Z., Ozolina V., 1974, Investigations of the Sun and Red stars, ed. A. Balklavs, Zinatve Riga, Vol. 2, 5

Alksne Z., Ozolina V., 1975, Investigations of the Sun and Red stars, ed. A. Balklavs, Zinatve Riga, Vol. 3, 29

Alksne Z., Ozolina V., 1976, Investigations of the Sun and Red stars, ed. A. Balklavs, Zinatve Riga, Vol. 4, 5

Alksne Z., Ozolina V., 1983, Investigations of the Sun and Red stars, ed. A. Balklavs, Zinatve Riga, Vol. 19, 40

Bachillar R., Gómez-González J., Bujarrabal V., Martín-Pintado J., 1988, A&A 196, L5

Benson P.J., Little-Marenin I.R., 1987, ApJ 316, L37

Booth R.S., Delgado G., Hagström M., Johansson L.E.B., Murphy D.C., Olberg M., Whyborn N.D., Greve A., Hansson B., Lindström C.O., Rydberg A., 1989, A & A 216, 315

Boothroyd A.I., Sackmann I.-J., 1988a, ApJ 328, 641

Boothroyd A.I., Sackmann I.-J., 1988b, ApJ 328, 653 (BS)

Boothroyd A.I., Sackmann I.-J., 1988c, ApJ 328, 671

Bujarrabal V., Gómez-González J., Bachillar R., Martín-Pintado J., 1988, A & A 204, 242

Bujarrabal V., Gómez-González J., Planesas P., 1989, A & A 219, 256

Cardelli J.A., Clayton G.C., Mathis J.S., 1988, ApJ 345, 245

Catchpole R.M., Feast M.W., 1985, in: Cool stars with excesses of heavy elements, Reidel, Dordrecht, p. 113

Chan S.J., Kwok S., 1988, ApJ 334, 362

Claussen M.J., Kleinmann S.G., Joyce R.R., Jura M., 1987, ApJS 65, 385

Daube I., Ozolina V., 1974, Investigations of the Sun and Red stars, ed. A. Balklavs, Zinatve Riga, Vol. 2, 14

Deguchi S., Nakada Y., Sahai R., 1990, A&A 230, 339

Eder J., Lewis B.M., Terzian Y., 1988, ApJS 66, 183

Epchtein N., Le Bertre T., Lépine J.R.D., 1990, A&A 227, 82

Epchtein N., Le Bertre T., Lépine J.R.D., Marques dos Santos P., Matsuura M.T., Picazzio E., 1987, A&AS 71, 39

Feast M.W., 1989, Evolution of peculiar red giant stars, eds. H.R. Johnson, B. Zuckerman, Cambridge University Press, p. 26

Forrest W.J., Merrill K.M., Russell R.W., Soifer B.T., 1975, ApJ 199, L181

Frogel J.A., Persson S.E., Cohen J.G., 1980, ApJ 239, 495

Fuenmayor F.J., 1981, Rev. Mex. Astron. Astrofis. 6, 83

Gezari D.Y., Schmitz M., Mead J.M., 1987, Catalog of Infrared Observations, 2nd edition. NASA reference publication 1196

Hacking P., Neugebauer G., Emerson J.P., Beichman C.A., Chester T.J., Gillett F.C., Habing H., Helou G., Houck J.R., Olnon F.M., Rowan-Robinson M., Soifer B.T., Walker D., 1985, PASP 97, 633

Herman J., Burger J.H., Pennix W.H., 1986, A&A 167, 247

Huggins P.J., Healey A.P., 1990, ApJ 346, 201

Ishida K., Weinberger R., 1987, A&A 178, 127

Joint IRAS Science Working Group, 1986, IRAS catalogues and Atlasses, Low Resolution Spectrograph (LRS), A&AS 65, 607

Joint IRAS Science Working Group, 1986, IRAS catalogues and Atlasses, Point Source Catalogue (PSC) (Washington: US Government Printing Office)

Joint IRAS Science Working Group, 1986, IRAS catalogues and Atlasses, Explanatory Supplement (Washington: US Government Printing Office)

Jones B., Merrill K.M., Puetter R.C., Willner S.P., 1978, AJ 83, 1437

de Jong T., 1989, A&A 223, L23

de Jong T., 1990, From Miras to Planetary Nebulae, eds. M.O. Mennssier, A. Omont, Editions Frontières, Gif sur Yvette p. 289

Jura M., 1986, ApJ 309, 732

Jura M., 1987, ApJ 313, 743

Jura M., Joyce R.R., Kleinmann S.G., 1989, ApJ 336, 924

Jura M., Kleinmann S.G., 1989, ApJ 341, 359

Kholopov P.N., Samus N.N., Frolov M.S., Goranskij N.A., Kireeva N.N., Kukarkina N.P., Kurochkin N.E., Medvedena G.I., Perova N.B., Shugarov S.Yu., 1985, General Catalogue of Variable Stars, 4th edition. Nauka, Moscow

Kleinmann S.G., 1989, Evolution of peculiar red giant stars, eds. H.R. Johnson, B. Zuckerman, Cambridge University Press, p. 13

Kleinmann S.G., Gillett F.C., Joyce R.R., 1981, ARA&A 19, 411

Kleinmann S.G., Sargent D.G., Moseley H., Harper D.A., Loewenstein R.F., Telseco C.M., Thronson H.A., 1978, A&A 65, 139

Knapp G.R., 1986, ApJ 311, 731

Knapp G.R., Morris M., 1985, ApJ 292, 640

Knapp G.R., Sutin B.M., Phillips T.G., Ellison B.N., Keene J.B., Leighton R.B., Masson C.R., Steiger W., Veidt B., Young K., 1989, ApJ 336, 822

Kukarkin B.V., Kholopov P.N., Artiukhina N.M., Fedorovich V.P., Frolovs M.S., Goranskij V.P., Gorynya N.A., Karitskaya E.A., Kireeva N.N., Kukarina N.P., Kurochkin N.E., Medvedeva G.I., Perova N.B., Ponomareva G.A., Samus N.N., Shugarov S.Yu., 1982, New Catalogue of Suspected Variable Stars. Nauka, Moscow

Kurtanidze O.M., Nikolashvili M.G., 1988, Afz 29, 470

Kurtanidze O.M., Nikolashvili M.G., 1989, Afz 31, 507

Kurtanidze O.M., West R.M., 1980, A&AS 39, 35

Kwok S., Bignell R.C., 1984, ApJ 276, 544

Lambert D.L., Hinkle K.H., Smith V.V., 1990, AJ 99, 612

Lattanzio J.C., 1989, ApJ 344, L25

Leahy D.A., Kwok S., Arquilla R.A., 1987, ApJ 320, 825

Le Bertre T., Deguchi S., Nakada Y., 1990, A&A 235, L5

Lequeux J., Jourdain de Muizon J., 1990, A&A 240, L19

Le Squeren A.M., Sivagnanam P., Dennefeld M., David P., 1991, A&A (in preparation)

Lindqvist M., Nyman L.-Å., Olofsson H., Winnberg A., 1988, A&A 205, L15

te Lintel-Hekkert P., 1990, PhD.-thesis. Leiden

Little-Marenin I.R., 1986, ApJ 307, L15

Little-Marenin I.R., Ramsey M.E., Stephenson C.B., Little S.J., Price S.D., 1987, AJ 93, 663

Lloyd Evans T., 1990, MNRAS 243, 336

Lundgren K., 1988, A&A 200, 85
MacConnell D.J., 1979, A&AS 38, 335
MacConnell D.J., 1982, A&AS 48, 355
MacConnell D.J., 1988, AJ 96, 354
Maehara H., Soyano T., 1987a, Ann. Tokyo Astron. Obs. 2nd series, Vol. 21, No. 3, 293
Maehara H., Soyano T., 1987b, Ann. Tokyo Astron. Obs. 2nd series, Vol. 21, No. 4, 423
Maehara H., Soyano T., 1988, Ann. Tokyo Astron. Obs. 2nd series, Vol. 22, No. 1, 59
Meadows P.J., Good A.R., Wolstencroft R.D., 1987, MNRAS 225, 43P
Meatheringham S.J., Maran S.P., Stecher T.P., Michalitsianos A.G., Gull T.R., Aller R.H., Keyes C.D., 1990, ApJ 361, 101
Merrill K.M., Stein W.A., 1976, PASP 88, 25
Milne D.K., Aller L.H., 1980, AJ 85, 17
Nercessian E., Guilloteau S., Omont A., Benayoun J.J., 1989, A&A 210, 255
Neugebauer G., Leighton R.B., 1969, Two Micron Sky Survey. NASA SP-3047
Nguyen-Q-Rieu, Epichtein N., Truong-Bach, Cohen M., 1987, A&A 180, 117
Nikolashvili M.G., 1987a, Afz 26, 209
Nikolashvili M.G., 1987b, Afz 27, 197
Noguchi K., Kawara K., Kobayashi Y., Okuda H., Sato S., Oishi M., 1981, PASJ 33, 373
Noguchi K., Maihara T., Okuda H., Sato S., 1979, PASJ 29, 511
Olofsson H., 1989, Evolution of Peculiar Red Giants, ed. H. Johanson, B. Zuckerman, Cambridge Univ. Press, p. 321
Olofsson H., Carlstrom U., Eriksson K., Gustafsson B., Willson L.A., 1990, A&A 230, L13
Olofsson H., Eriksson K., Gustafsson B., 1987, A&A 183, L13
Olofsson H., Eriksson K., Gustafsson B., 1988, A&A 196, L1
Olofsson H., Eriksson K., Gustafsson B., 1988, A&A 230, 405
Parthasarathy M., 1991, A&A 247, 429
Phillips J.P., 1989, Planetary Nebulea, ed. S. Torres-Peimbert, Kluwer, Dordrecht, p. 425
Price S.D., Murdock T.L., 1983, The revised AFGL Infrared Sky Survey Catalog, AFGL-TR-83-0161
Rana N.C., 1987, A&A 184, 104
Renzini A., Voli M., 1981, A&A 94, 175
Russell R.W., Soifer B.T., Willner S.P., 1978, ApJ 220, 568
Sanduleak N., Pesch P., 1988, ApJS 66, 387
Scalo J.M., 1986, Fundan. Cosmic. Phys. 11, 1
Schönberner D., 1989, Planetary Nebulae, ed. S. Torres-Peimbert, Kluwer, Dordrecht, p. 463
Skinner C.J., Griffin I., Whitmore B., 1990, MNRAS 243, 78
Slijkhuis S., 1990, From Miras to Planetary Nebulae, eds. M.O. Mennessier, and Omont, Editions Frontières, Gif sur Yvette, p. 312
Sopka R.J., Olofsson H., Johansson L.E.B., Nguyen-Q-Rieu, Zuckerman B., 1989, A&A 210, 78
Stephenson C.B., 1973, Publ. Warner and Swasey Obs., Vol. 1, No. 4
Stephenson C.B., 1985, AJ 90, 784
Stephenson C.B., 1989, Publ. Warner and Swasey Obs., Vol. 3, No. 2
Thronson H.A., Latter W.B., Black J.H., Bally J., Hacking P., 1987, ApJ 322, 770
Vader J.P., de Jong T., 1981, A&A 100, 124
Van der Veen W.E.C.J., 1989, A&A 210, 127
Van der Veen W.E.C.J., Breukers R.J.L.H., 1989, A&A 213, 133
Van der Veen W.E.C.J., Olofsson H., 1990, From Miras to Planetary Nebulae, eds. M.O. Mennessier, A. Omont, Editions Frontières, Gif sur Yvette, p. 139
Van der Veen W.E.C.J., Rugers M., 1989, A&A 226, 183
Volk K., Cohen M., 1989, AJ 98, 931
Walker H.L., Cohen M., 1988, AJ 95, 1801
Wannier P.G., Sahai R., 1986, ApJ 311, 335
Wannier P.G., Sahai R., Andersson B.-G., Johanson H.R., 1990, ApJ 358, 251
Westbrook W.E., Becklin E.E., Merrill K.M., Neugebauer G., Schmidt M., Willner S.P., Wynn-Williams C.G., 1975, ApJ 202, 407
Westerlund B.E., Azzopardi M., Breysacher J., 1986, A&AS 65, 79
Westerlund B.E., Azzopardi M., Breysacher J., Rebeirot E., 1990, From Miras to Planetary Nebulae, eds. M.O. Mennessier, A. Omont, Editions Frontières, Gif sur Yvette, p. 338
Whitelock P., 1985, MNRAS 213, 51p
Willems F.J., 1988a, A&A 203, 51
Willems F.J., 1988b, A&A 203, 65
Willems F.J., de Jong T., 1986, ApJ 309, L39
Willems F.J., de Jong T., 1988, A&A 196, 173
Wood P.R., Cahn J.H., 1977, ApJ 211, 499
Wood P.R., 1990, From Miras to Planetary Nebulae, eds. M.O. Mennessier, A. Omont, Editions Frontières, Gif sur Yvette, p. 67
Zuckerman B., Aller L.H., 1986, ApJ 301, 772
Zuckerman B., Dyck H.M., 1986a, ApJ 304, 394
Zuckerman B., Dyck H.M., 1986b, ApJ 311, 345
Zuckerman B., Dyck H.M., 1989, A&A 209, 119
Zuckerman B., Dyck H.M., Claussen M.J., 1986, ApJ 304, 401
Zuckerman B., Maddalena R.J., 1989, A&A 223, L20